Tu-AM-L7

THE PUTATIVE PLASTOCYANIN BINDING SITE IN *Chlamydomonas reinhardtii* CYTOCHROME F . ((J.G. **Fernandez-Velasco**, J. Zhou and R. Malkin)) Dept. Plant Biology, 461 Koshland Hall. Univ. of California. Berkeley, CA 94720.

The cluster of lysines proposed as the plastocyanin binding site in the cytochorome f of turnip (1) has a similar configuration in *C. reinhardtii* (2). Mutants of *C. reinhardtii* were prepared with altered electrical charge for lysines 58, 65, 66 (large domain) and 188, 189 (small domain) and the photooxidation of cyt f was measured. The reaction t1/2 for the wt is 0.20 ms (in the presence of stigmatellin and ionophores, at pH 7.0, Eh 0 mV, low ionic strength and 25°C). The reaction t1/2 for a first series of mutants analyzed are a) L188/L189 (0.38 ms), b) L188/L189/E58 (1.5 ms), c) L188/L189/E65 (2.2 ms), d) L188/L189/E66 (1.0 ms), e) E65/E66 (0.65 ms), f) E58/E65/E66 (1.5 ms), g) L188/L189/E65/E66 (2.1 ms) and h) L188/L189/E58/E65/E66 (1.5 ms). In all cases error is ca. $\leq \pm$ 15%. In contrast, the rates of cytochrome f re-reduction are very similar (t1/2 3-5 ms) in wt and all mutant strains. It is concluded that: 1) Lys residues from both the small and large domains are involved in the cytochrome fast oxidation but not, or only marginally, in the re-reduction from the FeS center. This is in agreement with the expected role for the altered amino acid residues as participants in the binding/electron transfer to plastocyanin. 2) All three Lys in the large domain are involved but they are not equivalent. 3) Synergistic effects between both domains exist, cf. a, e and g. 4) The degree of inhibition saturates by increasingly diminishing the net positive charge of the cluster. A reaction with t1/2 ca. 2.2 ms is the slowest attainable by neutralizing/inverting the cluster's positive charge complement. This could be explained either by a structural change of the site in the polymutated strains (cf. c vs. g and h), driven by the accumulation of Glu or by the elicitation of an alternative independent (artifactual?) reaction mechanism with plastocyanin. 1) Martinez, SE; Huang, D; Szczepaniak, A; Cramer, WA and Smith, JL (1994) Structure 2, 95-105 2) Berry, EA; Huang, L-s; Chi, Y; Zhang, Z; Malkin, R and Fernandez-Velasco, JG, this Meeting.

STRUCTURAL DETERMINANTS OF CALCIUM CHANNEL SIGNALING

T-PM-SymI-1 **W. Catterall, University of Washington**
Presynaptic Calcium Channels: Modulation and Role in Transmitter Release

T-PM-SymI-2 **T. Snutch, University of British Columbia**
Cross-talk Between PKC Up-regulation and G-protein Down-regulation of Calcium Channels

T-PM-SymI-3 **K. Campbell, University of Iowa**
Subunit Interaction Sites in Voltage-gated Calcium Channels

T-PM-SymI-4 **K. Beam, Colorado State University**
Cross-talk Between Voltage-gated and Intracellular-release Calcium Channels

AIDS AND ITS ASSOCIATED OPPORTUNISTIC INFECTIONS - DRUG DISCOVERY AND DEVELOPMENT

T-PM-SymII-1 **H. Ukwu, Merck Research Laboratories**
Anti-HIV Drugs - U.S. Regulatory Process

T-PM-SymII-2 **M. A. Navia, Vertex Pharmaceuticals, Inc.**
Structure-based Drug Design of HIV Protease Inhibitors - Tolerability, Bioavailability and Potency as Design Criteria

T-PM-SymII-3 **J. Sacchettini, Texas A&M University**
Alternative Strategies for Combatting Multi-Drug Resistance in Tuberculosis

T-PM-SymII-4 **D. R. Davies, NIDDK**
Structural Studies of the HIV Integrase

Tu-PM-A1

ELEMENTARY STEPS OF THE CROSS-BRIDGE CYCLE IN RABBIT SOLEUS FAST-TWITCH MUSCLE FIBERS

((Gang Wang and Masataka Kawai)) Dept of Anatomy, Univ of IA, IA City, IA 52242.

Elementary steps of the cross-bridge cycle were investigated with sinusoidal analysis in rabbit soleus fast-twitch fibers (FTF). The single fibers were activated at pCa 4.40, ionic strength 180 mM, 20°C, and the effects of MgATP (S) and phosphate (P, Pi) on three exponential processes were studied. The results are consistent with the following cross-bridge scheme:

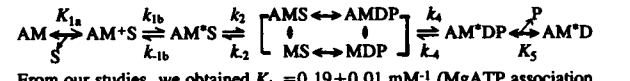

From our studies, we obtained K_{1a}=0.19±0.01 mM^{-1} (MgATP association constant), k_{1b}=572±30 s^{-1} (rate constant of ATP isomerization), k_{-1b}=276±27 s^{-1} (reverse isomerization), K_{1b}=2.2±0.3 (equilibrium constant), k_2=115±9 s^{-1} (cross-bridge detachment), k_{-2}=43±1 s^{-1} (reversal of detachment), K_2=2.7±0.2, k_4=28±1 s^{-1} (force-generation), k_{-4}=18±2 s^{-1} (reverse force generation), K_4=1.60±0.14, and K_5=0.10±0.03 mM^{-1} (Pi association constant). K_{1a} is 1/6 of that in rabbit soleus slow-twitch fibers (STF), indicating that MgATP binds to cross-bridges less tightly in soleus FTF than in soleus STF. These results indicate that cross-bridges of FTF are less resistant to ATP depletion than those of STF. The rate constants of the elementary steps are in general 5X of those in STF, but 1/5 of psoas. The individual equilibrium constants of the elementary steps in soleus FTF, soleus STF, and psoas fibers are similar. We conclude that the cross-bridge scheme is not any different among different fiber types.

Tu-PM-A2

EFFECT OF SARCOMERE LENGTH ON THE RATE OF TENSION REDEVELOPMENT AND CA^{2+} SENSITIVITY OF TENSION IN SLOW-AND FAST-TWITCH SKINNED SKELETAL MUSCLE FIBERS.

((K.S. McDonald, M.R. Wolff, and R.L. Moss)) Depts of Physiology and Medicine, University of Wisconsin Medical School, Madison WI 53706

Twitch tension falls with decreasing sarcomere length (SL) in striated muscle. One mechanism which may contribute to this phenomenon is SL-dependent change in crossbridge kinetics during isometric force development. We tested this idea by measuring the rate of force redevelopment (k_{tr}) as a function of sarcomere length in skinned slow and fast-twitch skeletal muscle fibers. In slow-twitch fibers, k_{tr} was 4.89±0.74 s^{-1} (n=12) during maximal activations at SL of ~2.30μm and fell to 3.94±0.66 when SL was decreased to ~2.00μm. During submaximal activations k_{tr} was lower at SL 2.00μm compared to SL 2.30μm in both slow- and fast-twitch skeletal muscle fibers. The decrease in k_{tr} over this SL range was greater in fast-twitch fibers (38% reduction) than in slow-twitch fibers (14% reduction). Ca^{2+}-sensitivity of tension, as assessed as the pCa for half-maximal activation (pCa_{50}) also decreased to a greater extent in fast-twitch fibers (ΔpCa_{50} of 0.24±0.07 pCa units) than in slow-twitch fibers (ΔpCa_{50} of 0.10±0.04 pCa units) when SL was reduced from ~2.30μm to ~1.85μm. Osmotic compression of both slow- and fast-twitch fibers at SL 2.00μm increased k_{tr} to values similar to those obtained at SL 2.30μm, indicating that the slower rate of tension redevelopment at short SL is due in part to the increase in interfilament lattice spacing associated with shorter SL. Together, these results suggest that length dependence of twitch tension is in part due to length dependence of isometric crossbridge kinetics, an effect mediated by interfilament lattice spacing.

Tu-PM-A3

KINETICS OF THIN FILAMENT ACTIVATION PROBED BY THE FLUORESCENCE OF IANBD-LABELED TROPONIN-I

((B. Brenner*, T. Kraft*, J.M. Chalovich#)) *Dept. of Clinical Physiology, Medical School Hannover, D-30625 Hannover, Germany; #Dept. of Biochemistry, East Carolina University, Greenville, NC 27858-4354, USA

We showed earlier that the fluorescence of troponin labeled on the TnI subunit with IANBD is sensitive to cross-bridge attachment to actin in addition to changes in [Ca^{++}]. This allows analysis of the kinetics of changes in thin filament activation in response to rapid variation of the fraction of strongly attached, force generating cross-bridges at constant [Ca^{++}]. For instance, changing from isometric to unloaded isotonic contraction reduces the fraction of strongly attached cross-bridges with a rate constant of >100 s^{-1} at all levels of Ca^{++}-activation. However, the rate of the fluorescence change of IANBD-TnI increased from about 10 s^{-1} to 80 s^{-1} with increasing Ca^{++} activation indicating that the fluorescence change is significantly slower than the rate of decrease in the fraction of strongly attached cross-bridges. This suggests that *when switching from isometric to isotonic steady state contraction*, the fluorescence change reports deactivation/reactivation kinetics of the thin filaments and not the kinetics of changes of occupancy of force-generating states. However, these fluorescence changes (upon changeover to isotonic steady state) were more than 10x faster than redevelopment of isometric force *in going from isotonic contraction back to isometric steady state contraction* with restretch of fibers back to their initial isometric sarcomere length. This suggests that, as we previously proposed, the slow time course of force redevelopment (and of the parallel change in IANBD-TnI-fluorescence) when switching back to isometric contraction is limited by isometric cross-bridge cycling kinetics and not by deactivation/reactivation kinetics of the thin filaments. Assuming that the changes in IANBD-TnI-fluorescence reflect changes in thin filament activation, our modeling shows that the observed behavior can be accounted for by a kinetic scheme that we had previously proposed for regulation of muscle contraction (Brenner, PNAS, 1988).

Tu-PM-A4

FORCE GENERATION IN SINGLE FROG SKELETAL MUSCLE MYOFIBRILS RAPIDLY ACTIVATED AT DIFFERENT CALCIUM CONCENTRATIONS.

((F. Colomo, S. Nencini, N. Piroddi, C. Poggesi & C. Tesi)) Dip.Scienze Fisiologiche, Università di Firenze, Viale Morgagni 63, 50134 Firenze, Italia.

Single myofibrils or thin bundles of 2-3 myofibrils 50-100 μm long prepared by homogenization of frog glycerinated tibialis anterior muscle were activated using a novel method which allows solution changes within 10-30 ms. The preparations were mounted horizontally between the lever arms of an isometric force transducer and a length control motor (Colomo et al., J. Physiol., 1994, 475, 347-350) in a temperature controlled trough filled with relaxing solution (pCa 8, 15 °C). Sarcomere length was set just above slack length (2.1-2.2 μm). Mounted myofibrils were continuously perfused by one of two parallel streams of solution jetted by gravity from a theta style glass pipette. Each pipette channel was connected to reservoirs filled with either relaxing or activating solutions of different calcium concentration (MgATP 3mM plus CP/CPK regenerating system). The perfusion system was firmly attached to a stepping motor that could be operated to cause rapid alternation of the stream flowed over the myofibril. When myofibrils were activated at pCa 4.75, tension rapidly rose to a maximal value of 376 ±21 kN/m^2 (n=16), with a half time of about 50 ms. The rate of force development seemed not affected by lowering the calcium concentration of the activating solution. The pCa/force relation obtained for single myofibrils from frog skeletal muscle was consistent with what reported for larger preparations: the threshold for active force generation resulted just above pCa 6 while 50% of maximal tension was attained at pCa 5.75.

Tu-PM-A5

REPRIMING OF THE WORKING STROKE FOLLOWING A STRETCH IN GLYCERINATED FIBERS OF RABBIT PSOAS MUSCLE

((Perry L. Sun, Jody A. Dantzig, Henry Shuman, and Yale E. Goldman)) Pennsylvania Muscle Institute, University of Pennsylvania, Philadelphia, PA 19104.

By 50 ms after a quick stretch of a contracting intact frog fiber, myosin heads regain their original conformation and the ability to execute a normal working stroke (Lombardi et al., *Nature* 374:553, 1995). Using rabbit skinned fibers, we investigated whether the rate of this "repriming" process depends on the phosphate (P_i) concentration. A conditioning stretch (amplitude 4-5 nm/half sarcomere (h.s.), arrow in fig.) was imposed during each contraction at 10°C, followed by a test release (amplitude 2-2.5 nm/h.s.) after a time Δt. Paired control releases from isometric (fig. inset) were applied during the contractions. In the figure, Δt ranged from 4-100 ms. The extent of quick tension recovery 3 ms after the test release was defined as **E** (fig. inset). For a test release imposed shortly after the conditioning stretch, **E** was smaller than control. As Δt lengthened, **E** increased exponentially with rate constant k_r to the control value. k_r was found to be ~40 s^{-1} at 0 added P_i, and ~60 s^{-1} at 5 mM P_i, much faster than the actomyosin ATPase rate. These rate constants match the rates of cross-bridge detachment and reattachment estimated from the tension recovery following the stretch (Dantzig et al., *Biophys. J.* 70:A126, 1996). The results suggest that repriming involves P_i binding to force-generating cross-bridges, and replacement by new attachments with the isometric conformation. Supported by NIH grant AR42333 and the MDA.

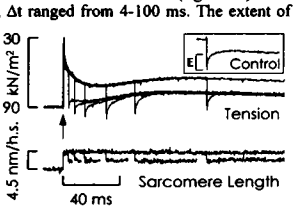

Tu-PM-A6

MYOSIN CROSS-BRIDGE AND ACTIN FILAMENT COMPLIANCE IN ACTIVE AND RIGOR MUSCLE

((M. Linari[1], I. Dobbie[2], M. Irving[2], N. Koubassova[1], M. Reconditi[1], G. Piazzesi[1] & V. Lombardi[1])) [1]Dip. Scienze Fisiologiche, Università di Firenze, 50134 Firenze, Italy, [2]The Randall Institute, King's College London, London WC2B 5RL, U.K. (Spon. by L. Castellani)

The compliance of the actin filament and myosin cross-bridges was investigated by measuring sarcomere compliance in the same muscle fibre both in an isometric contraction and in rigor in the sarcomere length range 2 to 2.15 μm (where the isometric tetanic tension is constant and sarcomere compliance depends solely on actin compliance). Experiments were done at 4 °C on single fibres dissected from tibialis anterior muscle of Rana esculenta. Rigor was obtained by MgATP depletion in the presence of BDM after permeabilization of the membrane with α-toxin. At each sarcomere length a train of five different sized length steps (range -3 to +5 nm per half-sarcomere, h.s.) was applied from an initial steady tension T_0, attained in the intact fibre by tetanic stimulation and in rigor by a slow ramp stretch of about 8 nm per h.s. The compliance of the actin filament, determined from the slope of the relation of the h.s. compliance versus sarcomere length, was ~2.4 nm/μm/T_0 in both the isometric tetanus and in rigor. This corresponds to a contribution to the total h.s. compliance of about 28 % in isometric contraction and 43 % in rigor. The relation between h.s. compliance and sarcomere length was shifted upward in the isometric tetanus compared to rigor indicating that, if all the heads are attached in rigor, no more than 46 % of the heads are attached in an isometric tetanus. This value would be reduced to 30 % if the myosin filament compliance were 2 nm/μm/T_0 as estimated from x-ray diffraction on whole muscle (Huxley et al., Biophys. J. 1994, 67:2411) and on single fibres (our unpublished results).

Supported by EC grant CHRX-CT94-0606, INTAS grant 93-576 and MRC (UK).

Tu-PM-A7

COMPLIANT REALIGNMENT OF BINDING SITES MEDIATES TENSION TRANSIENTS IN MUSCLE. ((**T.L. Daniel**, A.C. Trimble, and P.B. Chase)) Depts. of Zoology, and Physiology & Biophysics. Univ. of Washington, Seattle, WA 98195.

The presence of complaince in the lattice of filaments in muscle raises a number of concerns about how one accounts for force generation in the context of the cross–bridge cycle: binding site motions and mechanical coupling between cross–bridges confound more traditional analyses. To explore these issues, we developed a spatially explicit model of skeletal muscle contraction. With three states for the cross–bridge cycle, we used a Monte–Carlo simulation to compute the instantaneous forces throughout the filament lattice, accounting for both thick and thin filament distortions in response to cross–bridge forces. This approach is compared to more traditional mass–action kinetics models (as coupled partial differential equations) that assume inextensible filaments. We monitor as well, instantaneous force generation, ATP utilization, and cross–bridge dynamics in isometric conditions as well as length and phosphate transients. Three critical results emerge from our analyses : 1) there is a significant realignment of binding sites in response to cross–bridge forces, 2) this realignment recruits addtional cross–bridges, and 3) we predict mechanical behaviors that are consistent with experimental results for velocity, length and phosphate transients. Our results show that a model with simple rules for the cross–bridge cycle, with mechanical coupling through a lattice of compliant thin filaments, predicts transient responses that cannot arise in the absence of compliance. Moreover, we show that there are range of values for thin filament compliance that maximize force generation and the efficiency of contraction. Support: NSF IBN–9511681, NIH HL52558, SGI.

Tu-PM-A8

TRADING FORCE FOR SPEED: CROSS-BRIDGE KINETICS IN SUPERFAST FIBERS ((C.S. Cook, M. Ashley-Ross, D. Syme, Y. E. Goldman, L. C. Rome)) Pennsylvania Muscle Institute and Dept of Biology, Univ of Pennsylvania, Philadelphia PA 19104.

All vertebrate skeletal muscle fibers have similarly sized thick filaments and thus the same number of cross-bridges. Accordingly, the force per myofibrillar cross-section is nearly constant among skeletal fibers. An exception appears to be superfast muscles which generate very low forces. We have examined the properties of the superfast toadfish swimbladder muscle (SB; used to make a 200 Hz "boatwhistle" mating call) and compared it to that of toadfish red and white swimming muscles. In maximally activated skinned fibers, the force generated per myofibrillar cross-section by SB is only 56 kN/m^2 compared to 150 and 228 kN/m^2 for the red and white muscles respectively. Low force production could result from either 1) few attached cross-bridges or 2) low force per attached cross-bridge. To determine the proportion of attached cross-bridges, we compared the stiffness in the active fibers to that in rigor. The active to rigor stiffness ratios for red and white fibers were ~0.75; however, that for the SB was only 0.19. Accounting for the compliance residing in the myofilaments (50% during rigor), these ratios suggests that 60-70% of the cross-bridges were attached in the red and white fibers during contraction (similar to other fiber types), but only ~10% of the cross-bridges were attached in SB. Dividing force by the number of attached cross-bridges gives similar values for force per cross-bridge in all 3 fiber types. *Why do swimbladder fibers have so few attached cross-bridges?* By combining the stiffness with the isometric ATPase rate, we found that the cross-bridge detachment rate constant (g) was 274 s^{-1} while the attachment rate constant (f) was 32 s^{-1}. Whereas in other muscles previously studied the $f \geq g$, in SB $f << g$, resulting in few attached cross-bridges. The extraordinary speed of the SB's cross-bridge kinetics was further demonstrated by the rate of force development (k_{dev}) following release of caged Ca^{2+} (NP-EGTA). k_{dev} ($= f + g$) was 30, 81, and 440 s^{-1} for the red, white and SB respectively. In conclusion, in superfast fibers f doesn't appear able to keep pace with the high g required for fast relaxation. Thus, the number of attached cross-bridges is low which results in low force production. Supported by NIH AR42333 & AR38404, NSF IBN95.

Tu-PM-A9

IS THE ADP RELEASE STEP OF THE SMOOTH MUSCLE CROSS-BRIDGE CYCLE ASSOCIATED WITH FORCE GENERATION? ((**Jody A. Dantzig**, Robert J. Barsotti*, Scott A. Manz, H. Lee Sweeney, and Yale E. Goldman)) Pennsylvania Muscle Institute, University of Pennsylvania, Philadelphia, Pennsylvania, 19104 and *Bockus Research Institute, The Graduate Hospital, Philadelphia, Pennsylvania, 19146.

The light chain domain of smooth muscle myosin subfragment-1 (sm-S1) bound to actin tilts upon release of ADP[1,2] producing a ~ 3.5 nm axial motion of the head-rod junction. If this motion contributes significantly to the power stroke, rigor tension in smooth muscle should decrease substantially in response to the binding of MgADP. To test this prediction, we monitored the mechanical properties of permeabilized bundles of chicken gizzard muscle cells in rigor and in the presence of MgADP. Any residual bound ADP in rigor was minimized by incubation in Mg^{2+}-free or apyrase containing rigor solution. All rigor and ADP solutions contained 250 μM AP_5A, 20 μg/ml hexokinase and 200 mM glucose. MgADP (≥ 1 mM) was added by exchange in a solution with the same ionic strength and free Mg^{2+} as the rigor solution. Adding MgADP caused rigor tension to *increase* slightly (1.6 ± 0.6 %, n = 35 ± SEM) and in-phase 500 Hz stiffness to decrease (7.0 ± 1.0 %). The changes in force and stiffness were reversible and did not depend on ionic strength from 50 to 200 mM nor on the phosphorylation state of myosin. Our results suggest that the axial motion observed with acto.sm-S1 upon release of ADP[1,2] is not associated with a force generating transition in smooth muscle. This apparent discrepancy may be explained if geometrical constraints of the contractile filament array in the smooth muscle cell alter the motions of the myosin heads. Supported by NIH grants HL15835 to the P.M.I., AR35661 to H.L.S., and HL40953 to R.J.B.

[1]Whittaker *et al., Nature* 378:748, 1995., [2]Gollub *et al., Nature Struc. Biol.* 3:796. 1996.

PROTEIN STRUCTURE AND FUNCTION

Tu-PM-B1

ISOERGONIC COOPERATIVITY IN GLUTAMATE DEHYDROGENASE COMPLEXES; A NEW FORM OF ALLOSTERY. ((**Harvey F. Fisher** and Jon Tally)) VA and U. of Kansas Medical Centers, Kansas City, MO 64128

Homotropic allosteric cooperativity is currently defined in free energy terms involving order of magnitude differences in Kb's for successive steps in the binding of a ligand to the various sites of an oligomeric protein. Glutamate dehydrogenase shows no significant evidence of cooperativity as judged by this criterion. However, isothermal calorimetric titrations of the heats of formation of a variety of binary and ternary complexes of this enzyme show striking patterns of deviation from ideality. The apparent contradiction between these two findings requires the formulation of a new theoretical basis. Analysis of the isothermal binding curves indicate variations of an alternating series of enthalpy driven-entropy compensated and entropy driven-enthalpy compensated steps. The basic element of our proposed theory is our previous finding that the binding of NADPH to the enzyme involves the two-step process: E⇌E′⇌E-NADPH, where E⇌E′ represents a poised equilibrium between a high and a low ΔH° form and an exothermic binding step. We have shown that this mechanism generates the ΔCp effects observed in this system, accounts for the large variation in thermal stability between the various enzyme complexes, and plays a role in the transduction of ligand-binding energy into catalytic driving force. The introduction of such a feature into a standard multisite binding scheme, assuming only simple changes in the E⇌E′ steps, is sufficient to account for all observed phenomena. (Supported by the Dept. of Veterans Affairs and the NSF)

Tu-PM-B2

PROTON SWITCH AT THE BINUCLEAR CENTER OF CYTOCHROME C OXIDASE ((**Tapan K. Das***, David M. Mitchell#, Farol L. Thomson#, Robert B. Gennis#, Denis L. Rousseau*)) *Department of Physiology and Biophysics, Albert Einstein College of Medicine, NY 10461; #School of Chemical Sciences, University of Illinois, IL 61801

Cytochrome *c* oxidase (CcO), the terminal enzyme complex of the respiratory chain has a binuclear (heme a_3-Cu_B) catalytic site where oxygen is reduced to water. The electron transfer in this enzyme molecule is coupled to proton translocation. We have shown recently that the binuclear site of CcO from *Rb. Sphaeroides* possesses multiple conformations at neutral pH, based on their distinctly different Fe-CO stretching modes in the resonance Raman spectra. The pH-dependence of the two conformations (α and β) shows a reversible transition in the pH-range of 6-9. It has been proposed that these conformers result from structural changes in the distal pocket. A change of pK of some ionizable groups in the vicinity of the binuclear site may be functioning as the proton switch during the enzymatic cycle. Alteration of the pK could be induced by the potential generated across the mitochondrial membrane. The conformational transition induced by pH, however, is of a different nature in the bovine CcO. The β form is minimally populated near neutral pH but dominates over the α form at other pHs, just the opposite of the behavior in the bacterial enzyme. The structural difference in the vicinity of the binuclear center between the bovine and bacterial CcO will be discussed.

Tu-PM-B3

THE STRUCTURES OF CALMODULIN AND A FUNCTIONAL MYOSIN LIGHT CHAIN KINASE IN THEIR COMPLEX: A STUDY USING SMALL-ANGLE NEUTRON SCATTERING WITH CONTRAST VARIATION((**J.K.Krueger**, G. A. Olah, and J. Trewhella)) Los Alamos National Laboratory, Los Alamos, NM 87545. ((Gang Zhi and J. T. Stull)) Dept. Physiol., UT Southwestern Medical Center, Dallas TX 75235.

We will present structural information on the conformations and relative dispositions of $4Ca^{2+}$•calmodulin (CaM) and a fully functional truncate of skeletal muscle myosin light chain kinase (tSkMLCK) within the activated complex. Structural data on complexes of CaM with functional enzymes have been elusive due to the difficulties presented by the sizes, solubilities and stabilities of the intact enzymes for NMR or crystallographic studies. Our approach has been to use neutron scattering to study CaM•tSkMLCK in solution. This approach involves taking advantage of the large differences in neutron scattering lengths between hydrogen and deuterium by measuring neutron scattering of tSkMLCK bound to a specifically deuterated CaM at several H_2O:D_2O solvent ratios ("contrast variation"). For some time neutron scattering with contrast variation has been discussed in terms of its potential as a structural biology tool, and in a few cases it has been applied protein/protein and protein/DNA interactions. The results to date have been relatively modest due primarily to the limitations in available neutron fluxes. Recent upgrades of neutron sources and instrumentation have yielded gains in neutron fluxes that have enabled us to complete the contrast variation experiment on the CaM•tSkMLCK complex at the low protein concentrations that are frequently a limitation for neutron studies of biomolecular complexes.

Tu-PM-B4

DOCKING OF THE PROLACTIN RECEPTOR PROLINE-RICH MOTIF (PRM) TO FKBP12: IMPLICATIONS FOR CYTOKINE RECEPTOR SIGNALING ((**K.V. Soman**, B.A. Hanks, H. Tien, K.D. O'Neal, M.V. Chari and J.D. Morrisett)) Departments of Medicine and Biochemistry, Baylor College of Medicine, Houston, TX 77030. E-mail: ksoman@bcm.tmc.edu

A conserved proline rich motif (PRM) in the cytoplasmic domain of cytokine receptors has been suggested to be a signaling switch regulated by the action of the FKBP family of peptidylprolyl isomerases [O'Neal et al, 1995, Ann. N.Y. Acad. Sci., 766, 282]. We have docked the prolactin receptor PRM (Ile^1-Phe^2-Pro^3-Pro^4-Val^5-Pro^6-Gly^7-Pro^8) to the ligand binding site of FKBP12. The procedure involved conformational search restricted by NMR restraints [O'Neal et al., Biochem. J., 315, 833-844, 1996], energy minimization of the octapeptide conformers so obtained, template-based docking of a selected conformer to FKBP12, and energy refinement of the resulting complex. The template used was the crystal structure of a cyclic FK506-peptide hybrid bound to FKBP12. Val^5-Pro^6 of the PRM was taken to be the biologically relevant *Xaa-Pro* bond. The docked conformer is stabilized by two internal hydrogen bonds: $N^7H^7 \rightarrow O^4$ and $N^2H^2 \rightarrow O^8$, and two intermolecular ones: Ile_{56}:N-H→O=C:Pro^6 and Tyr_{82}:O-H→O=C:Gly^7. It features a Type I β-turn and has extensive hydrophobic contacts with the FKBP12 binding surface. The observed interactions support the hypothesis that FKBP12 catalyzes *cis-trans* isomerization in the PRM, and suggests a significant role for it in signal transduction.

Tu-PM-B5

USE OF LIGAND BINDING ENERGY: A STRUCTURAL VIEW

((C. J. Ritz-Gold)) Center for Biomolecular Studies, Fremont, CA 94536.

Ligand binding energy is used to perform two important functions: In typical enzymes, it is used to reduce the activation energy of the catalyzed reaction. In allosteric enzymes, receptors, and transducing systems, it is used to induce endergonic allosteric transitions. In both cases, the overall process is thought to involve two basic steps: 1) Energy storage - trapping of binding energy supplied from an external source; 2) Energy recovery - harnessing this stored energy to induce strain in the substrate molecule or to induce the allosteric transition. However, a detailed understanding of these two basic steps is still lacking.

Here we seek physical insight into the use of binding energy in protein molecules by looking at a ligand-induced allosteric transition from a structural point of view. The protein molecule is represented as a chain of coupled two-state (double-well) segments, and the allosteric transition as a displacive transformation. Also, fulfillment of latent binding interactions is represented as a chemical reaction taking place within an ordered medium (J.M. McBride et.al., Science, 234, 830, 1986). We find that: In the energy storage step, initial steric misfit between ligand and binding site first leads to input of chemical potential energy to the system. Then, the fulfillment of latent interactions and the (T)->[R] transition of the binding site region lead to generation of a strained [R]/(T) interface and thus, to storage of strain energy in the protein molecule. In the recovery step, this strain energy is released and harnessed to drive the (T)->[R] transition of the rest of the molecule. We conclude that looking at the use of ligand binding energy in protein molecules from a structural point of view can yield new physical insights into this important process.

Tu-PM-B6

PROTEIN ORGANIZATION IN ELECTRON TRANSFER PROTEINS: COMPUTATIONAL STUDIES OF IRON-SULFUR PROTEINS. (Robert B. Yelle, **Brian W. Beck** and T. Ichiye)) Department of Biochemistry/Biophysics, Washington State University, Pullman, WA 99164-4660.

The protein itself in electron transfer proteins plays many roles: a scaffold to hold the redox site, a binding site for redox partners, and an electrostatic environment for the redox site. Understanding the latter is the focus of these studies. Although charged side chains would seem to be most important in electrostatic studies, it appears that the polar contributions of the backbone, polar side chains and solvent play an important role. For instance, one obvious way that an electron transfer protein controls the environment is by excluding solvent (normally water, which is highly polar) from the redox site, thus providing a low dielectric environment. However, from our studies of Fe-S proteins, the protein is also highly polarized around the redox site, even more so than could be expected based on the net charge of the redox site. Thus, these proteins are better able to accept an electron than a redox site analog in a solvent with a dielectric constant equivalent to that of the protein. Moreover, this polarization is a general effect due to many residues rather than a few key residues. Since this type of effect has also been seen in the photosynthetic reaction center, it may be a general phenomena in electron transfer proteins. The degree of polarization for an environment of a given dielectric can be predicted by linear response theory so measures of the nonlinearity of the environmental response calculated from molecular dynamics simulations will be described. The protein folding aspects will also be discussed.

Tu-PM-B7

COORDINATION OF MG-MESOPORPHYRIN TO THE HEME POCKET OF HRP.((E.Balog, R.Galantai, K.Kis-Petik, **J.Fidy**, M.Koehler*, J.Friedrich*)) Inst. Biophys. Semm. Univ. Med. Budapest, H-1444, P.O.Box263, *Phys. Inst. Univ. Bayreuth, Bayreuth, D.

There is experimental evidence that the protein matrix may represent special constraints for the structure of embedded prosthetic groups as for the heme in hemoproteins. The doubly degenerate lowest energy excited states in D_{4h} symmetry metal porphyrins may be sensitive spectroscopic markers for the presence of symmetry breaking interactions in the environment of the molecule. In this work, the Q band of Mg-Mesoporphyrin in reconstituted HRP has been studied by low temperature broad band and high resolution absorption and fluorescence spectroscopic methods to elucidate the interactions that lead to the multiple band feature of this range when absorption spectra are measured. It has been shown that the presence of the protein crevice around the porphyrin lifts the degeneracy of the electronic transition and a pronounced Qx-Qy splitting results. Spectral hole burning studies of the multiple Q(0,0) bands unravel that besides this splitting, multiple band feature also arises from the presence of various Mg-MP structures coordinated to the heme pocket in the protein. By the same methods, the structural effect of binding an aromatic hydrogen donor, naphthohydroxamic acid has also been studied. After addition of NHA, only one single conformer of Mg-MP could be identified in HRP, and a significant increase in the extent of Qx-Qy splitting was seen. The bulk compressibility of the protein was not affected by binding. Thus the enzyme function of HRP is regulated by changing the symmetry of the pocket and the coordination of the prosthetic group. (Supported by the German-Hungarian S&T program no. 78, and Hung. grants FEFA 265, 412, 693)

Tu-PM-B8

DISTRIBUTION OF ELECTROSTATIC FIELD AROUND BIOLOGICAL MOLECULES STUDIED BY METHODS OF SPIN-PROBES AND NMR. ((G.I.Likhtenshtein, I. Vaisbuch, I. **Adin**, A. Shames*, R. Glaser)) Departments of Chemistry and Physics*, Ben-Gurion Unversity of the Negev, P.O.B. 653 , Beer-Sheva 84105, Israel

Electrostatic interactions play a key role in the structure and function of biological molecules. For the study of the distribution of local electrostatic fields around definite protons of functional groups in biological molecules we have developed two new independent experimental approaches. The first approach relies on the quantitative measurement of the contribution of nitroxide probes of different charges to the spin-lattice relaxation rate ($1/T_1$) of protons in the molecule of interest, followed by calculation of local electrostatic charges useing the classical Debye equation. The application of the method to aminoacids (glycin, lysin, histidin, and aspartic acid) in solution allowed us to estimate effective charges in the vicinity of individual protons in a good agreement with theoretically expected values. The second approach was the developement of a method named "spin label-spin probe" proposed by one of us in 1972. The method is based on the effect of electrostatic charges of spin-probes on the frequency of their encounters with paramagnetic complexes in solution, which is monitored by measurment of the paramagnetic contribution of the complexes to the spin-spin relaxation time of the nitroxide by the ESR technique. To establish the distribution of the electrostatic field in the vicinity of the heme group of cytochrome c and myoglobin we invstigated the effect of paramagnetic ferricytochrome c (Fe^{3+}cyt c) and ferrimyoglobin (Fe3+Mb) on the broadening of line width of the ESR signal of nitroxide probes of different charges . This allowed us to calculate rate constants of spin exchange which are proportional to the frequency of encounters and then by using Dedye theory to estimate the value of local electrostatic charges at close proximity to the protein active centres. Data presented in this work validated realability of the proposed approaches and permitted to discuss the biochemical significance of electrostatic effects in the given systems .

Tu-PM-B9

NOS ISOFORMS HAVE DISTICT SUBSTRATE BINDING SITES ((B. Fan[1], J. Wang[2], D. J. Stuehr[3] and D. L. Rousseau[1])) [1]Department of Physiology and Biophysics, Albert Einstein College of Medicine, Bronx, NY 10461; [2]Pharmaceutical Division, Ciba-Geigy Corporation, Summit, NJ 07901; [3]Department of Immunology, NN-1, The Cleveland Clinic, Cleaveland, OH 44195.

Due to the sensitivity of CO related modes to the protein environment, differences in the spectroscopic properties of the CO unit can be used to deduce structural information about its surroundings. The resonance Raman of the substrate bound form of the CO-adducts of three NOS isoforms have been measured. While the $\nu_{Fe\text{-}CO}$ was observed at 503 cm^{-1} for b-NOS, this mode is observed at 513 cm^{-1} for e-NOS and i-NOS. Although large differences in $\nu_{Fe\text{-}CO}$ are observed, a very similar $\delta_{Fe\text{-}C\text{-}O}$ frequency was observed for all three isoforms between 565-567 cm^{-1}. The difference in the $\nu_{Fe\text{-}CO}$ frequency and similarity in $\delta_{Fe\text{-}C\text{-}O}$ indicates that significant differences in polarity in the heme and/or substrate binding environment exists between b-NOS and the other two isoforms but a similar binding geometry is retained. Two mechanisms are proposed to account for these observations. A simple calculation based on the separation of a fractional positive charge on the arginine from the CO indicates that between these isoforms, the substrate position differs by about 1 angstrom. Different positive charge shielding may be a alternative explanation for these observations. This structural difference may serve as a basis for selective inhibitor binding.

Tu-PM-B10

SANS Studies of the Thermal Stability of the Double-Ring Structure of *E. coli* GroEL Chaperonin in Solution

((**P. Thiyagarajan**[1], Chwen-Yuan Ku[1], Elsie Quaite-Randall[2] and Andrejz Joachimiak[2])) [1]Intense Pulsed Neutron Source, [2]Center for Mechanistic Biology, Argonne National Laboratory. 9700 S. Cass Ave , Argonne, IL 60439, USA.

Chaperonins are essential proteins that assist in protein folding and in protecting cellular proteins against thermal aggregation. The x-ray crystal structure of GroEL chaperonin (Braig, K et al., *Nature* 371, 261-264, 1994) revealed that it exists as a complex of 14 subunits assembled into two 7-member rings that stack back to back (double-ring). Our previous SANS studies (Thiyagarajan, P. et al., *Structure*, 4, 79-88, 1996) demonstrated that the solution structure of GroEL is similar but not identical to that from the x-ray data and there exists an equilibrium between the double rings, single 7-subunit rings and individual subunits. To understand the effect of temperature on the stability of the double-ring structure, SANS studies were made on the GroEL solutions in D_2O in a temperature range of 10 to 75°C, both in the presence and absence of ADP. In the absence of ADP, the GroEL solution contains dimers and trimers of double-rings (in equilibrium) stacked end-to-end in the temperature range 10-50°C, and higher order aggregates of double-rings at 65 °C. At 75 °C the double-ring structure collapses into monomers which lead to aggregation of a different kind. In the presence of ADP, no dimers of double-rings were observed. Furthermore, ADP lowers the thermal stability of the double-ring structure such that they start to break down at 65 °C into subunits which form aggregates.

This work was supported by U.S. DOE, Contract # W-31-109-ENG-38 with University of Chicago .

K CHANNEL GATING I

Tu-PM-C1

HIDDEN COMPONENTS AND HIDDEN DEPENDENCIES DETERMINED FROM TWO-DIMENSIONAL (2-D) DWELL-TIME DISTRIBUTIONS FROM SINGLE BK CHANNELS IN RAT SKELETAL MUSCLE. ((**Karl L. Magleby**, Ricardo A. Bello, and Brad S. Rothberg)) Department of Physiology and Biophysics, University of Miami School of Medicine, Miami, FL 33101

Correlations between the durations of adjacent open and shut intervals in single channel recordings can provide insight toward identifying ion channel gating mechanisms. The purpose of the present study was to quantify the correlation information. Currents were recorded from single BK channels with the patch clamp technique from patches excised from primary cultures of rat skeletal muscle. The durations of adjacent open and shut intervals were measured, and the intervals pairs were log-binned to form 2-D dwell-time distributions. The 2-D distributions were then fitted with sums of 2-D exponential components to determine the open and shut time constants and volume describing each component. The 2-D dwell-time distributions for the examined BK channels were described by 2-D components determined by all possible combinations of 3-4 different open and 5-7 different shut time constants. Thus, the distributions could contain up to 28 (4 open x 7 shut) individual 2-D components. The 2-D fitting technique occassionally identified hidden components, and hence, hidden dependencies, that were not apparent when open or shut interval distributions were fitted separately. The dependencies indicated which interval pairs were in excess and which were in deficit over that expected for random pairing of intervals (Song and Magleby, 1992). This 2-D information provided direct insight into the connections among the kinetic states underlying the gating. Supported by grants from the NIH and Muscular Dystrophy Association.

Tu-PM-C2

GATING MECHANISMS FOR SINGLE BK CHANNELS DETERMINED USING Q-MATRIX FITTING OF TWO-DIMENSIONAL DWELL-TIME DISTRIBUTIONS. ((**Brad S. Rothberg**, Ricardo A. Bello, and Karl L. Magleby)) Dept. of Physiol. and Biophysics, Univ. of Miami School of Medicine, Miami, FL 33101

Distributions of adjacent open and shut interval durations obtained from single channel recordings can be used to discriminate between possible ion channel gating mechanisms (Weiss and Magleby, 1990). Such 2-D distributions can be calculated from discrete-state Markov models of channel gating using Q-matrix methods (Fredkin, Montal, and Rice, 1985). The purpose of the present study was to estimate rate constants and rank models for the gating of BK channels by fitting 2-D distributions using 2-D Q-matrix calculations and maximum likelihood techniques. Currents were recorded from single BK channels with the patch clamp technique from patches excised from primary cultures of rat skeletal muscle. The durations of adjacent open and shut intervals were measured, and the interval pairs were log-binned to form 2-D dwell-time distributions. The 2-D distributions were then fitted with sums of 2-D exponential components to obtain estimates of the minimum numbers of open and shut states involved in the gating. 2-D Q-fitting was then applied to determine the most likely set of rate constants for several different proposed gating mechanisms. The constraints imposed by fitting a 2-D distribution from a single data set could distinguish among different models that were not separable by conventional 1-D methods, since the 2-D fitting forces the kinetic scheme to account for the correlations between adjacent interval durations. The 2-D distributions were described well by kinetic schemes containing 3-4 open states and 5-7 closed states. Supported by grants from the NIH and MDA.

Tu-PM-C3

EVIDENCE FOR MULTIPLE OPEN STATES IN Kv1.5 GATING. ((T.C. Rich and **D.J. Snyders**)) Vanderbilt University School of Medicine, Nashville, TN 37232

The kinetic properties of hKv1.5 expressed in L-cells were studied to develop a comprehensive gating model. Upon depolarization, the activating hKv1.5 currents exhibited a delay but no Cole-Moore shift was observed. The subsequent time course of activation was best described by a sum of two exponentials (at +50 mV: $\tau_1 \approx 2$ ms, $\tau_2 \approx 11$ ms, A_2=15%). To test whether this slow component reflected recruitment of channels from a 'hesitant' closed state, we analyzed hKv1.5 activation following 5 s voltage steps near the threshold for activation. Interestingly, this reduced the amplitude of the fast component while the slow component persisted, suggesting that the latter reflected a redistribution between open states. As the duration of the preceding depolarization was increased, the biexponential time course of deactivation between -80 to -30 mV became progressively slower due to a change in the relative contributions of fast and slow components; such behavior is not expected for deactivation from a single open state. The time constants for induction of and recovery from slow inactivation displayed little temperature or voltage dependence, but the extent of inactivation increased substantially with temperature, and long depolarizations (20 s) slowed the apparent rate of subsequent recovery from inactivation. A global fit procedure (SCoP) simultaneously using data sets covering activating, inactivating and deactivating currents between -80 to +60 mV failed to converge unless more than one open state was incorporated in the gating model. Thus, both the data and the modeling strongly suggest the existence of multiple open states for hKv1.5. Supported by grants HL-47599, HL-46681 and an AHA Grant-in-Aid.

Tu-PM-C4

A *C. ELEGANS EGG-LAYING ABNORMAL (EGL-36)* MUTATION ENCODES A SHAW-TYPE POTASSIUM CHANNEL WITH ALTERED ACTIVATION. ((**A. Wei***, D. Johnstone[+], J. Thomas[+], and L. Salkoff*)) *Department of Anatomy and Neurobiology, Washington University School of Medicine, St. Louis, MO 63110 and [+]Department of Genetics, University of Washington, Seattle, WA 98195.

At least three distinct genetic loci encode Shaw-type potassium channels in *C. elegans*, as revealed by the *C. elegans* genome sequencing project. Mutations at one of these loci were found to be associated with the behavioral mutant *egg-laying abnormal (egl-36)*. The *egl-36* phenotype is characterized by abnormal retention of eggs, which is thought to result from altered excitability of the egg-laying muscles. Wild-type and mutant Shaw-type potassium channels encoded by the *egl-36* locus were cloned and expressed in *Xenopus* oocytes. Wild-type *egl-36* Shaw cRNA expressed non-inactivating currents similar to *Drosophila* Shaw, with slow activation kinetics and a relatively depolarized G-V relationship (V_{50} = +70 mV). In contrast, mutant channels produced by the dominant allele, *egl-36(n2332)*, expressed currents with dramatically altered activation properties. The G-V relationship of mutant channels was shifted -50mV relative to wild-type. In addition, mutant channels activated with nearly instantaneous kinetics. These altered properties could increase resting potassium conductance at hyperpolarized potentials, thus lowering the excitability of muscle cells. The *egl-36(n2332)* mutation is a single-base missense mutation in S6 which substitutes serine for the highly conserved proline 439. These results support models which propose an involvement of S6 in potassium channel activation. Because *C. elegans* will tolerate potassium channel mutations which may otherwise be lethal in more complex metazoans, it may be uniquely suited for genetic studies which address the relationship of particular potassium channels to specific behaviors and physiological functions.

Tu-PM-C5

MODIFICATION OF *SHAKER* POTASSIUM CHANNEL GATING BY DEUTERIUM OXIDE ((**D. Starace** and F. Bezanilla)) Departments of Physiology and Anesthesiology, UCLA, Los Angeles, CA, 90095

We have examined the access of the gating machinery of the *Shaker* potassium channel to the bulk solution by replacing water in the recording solution with deuterium oxide (D_2O). Applied both externally and internally, D_2O substitution slowed the kinetics significantly of ON and OFF gating charge movement in the non-conducting and fast inactivation-removed mutant, H4IR[W434F]. The temperature dependence of the effect of D_2O as compared to H_2O was studied in order to differentiate between an isotopic and solvent effect. The temperature dependence of the modification of gating kinetics by D_2O has not yet resolved whether the action of D_2O arises primarily from isotopic exchanges or alteration of the solvent structure. The voltage dependence of gating charge movement and the maximum charge moved was unaffected when the channel was maintained in a noninactivated state. However, when the channel was driven into its slow, C-type inactivated sate by holding at 0 mV, the voltage dependence of subsequent gating charge movement in D_2O was shifted by 5-10 mV to more hyperpolarized potentials, relative to H_2O. This shift is consistent with an increase of the interaction energy between activation charge and another part of the protein, which is thought to mediate C-type inactivation. Since published studies have found no change in the kinetics of gating currents by D_2O, it has been generally believed that the gating machinery of sodium and potassium channels is not exposed to the solvent. On the contrary, our results are consistent with the view that the gating segment has access to D_2O and opens the prospect of exploring possible solvent filled crevices in the channel protein by manipulation of the bulk solution in combination with alteration of the channel. Supported by NIH GM30376.

Tu-PM-C6

VOLTAGE DEPENDENCE OF THE EARLY EVENTS IN VOLTAGE GATING ((**E. Stefani** and F. Bezanilla)) Departments of Anesthesiology and Physiology, UCLA, Los Angeles, CA 90095-1778

We have reported that in the non-conductive *Shaker B* K^+ channels with the inactivation ball removed (Shaker B IR, W434F), gating currents show a large initial component that rises as fast as the settling time of the capacity transient (~ 2 μs) and decays with a time constant of about 8 μs at 0 mV at room temperature. This fast component is present at the ON for depolarizing pulses and at the OFF for repolarizations. Effective bandwidth was 200 kHz and the data were sampled at 5 MHz. To characterize the voltage dependence of the early component we investigated the adequacy of the subtracting protocol. Macropatches from oocytes expressing *Shaker B* K^+ channels were maintained at -90 mV and pulses ranging from +30 to -400 mV were delivered. The early component remained unmodified with positive-going subtracting pulses (P/1 or P/-1) from a subtracting holding potential of 20, 50, and 100 mV. The Q-V curve of the early component has a shallow voltage dependence saturating near 0 and towards -400 mV with an effective valence of about 0.5 e_0 and a half activation potential of -160 mV. The early component is about 0.06 of the total charge. Assuming 12 e_0 per channel, the expected effective valence is 0.72 e_0, which is close to the experimental value for a simple Boltzmann fit of 0.5 e_0. The charge rearrangement of the fast component is not strictly sequential with the main charge movement because its magnitude and time course at the end of a depolarizing pulse are unaffected with manipulations that change the proportion of the charge in the open state, such as pulse duration, internal TEA or the ball peptide in wild type channels. The fast event could be a charge displacement that moves independently of the main gating charge or it could be the result of charge rearrangements of the main gating charge within wells in a diffusion regime (Sigg and Bezanilla, this meeting). Supported by NIH grants GM52203 and GM30376 .

Tu-PM-C7

CHARACTERIZING FAST AND SLOW EVENTS IN ION CHANNEL ACTIVATION WITH A DIFFUSION PROCESS ((**D. Sigg** and F. Bezanilla)) Departments of Physiology and Anesthesiology, UCLA, Los Angeles, CA, 90024

We have experimented with modeling gating charge movement in ion channels as diffusive motion of the generalized voltage sensor. The usual method of using chemical transition state theory (TST) to describe gating current kinetics is inadequate in describing early ($\tau \approx 10$ μsec) components of the gating current[1]. By specifying the gating charge displacement q as a reaction coordinate for protein conformation along the activation pathway, gating current kinetics arise from Brownian motion of q across a free energy landscape. Mean gating currents are computed through a simple numerical method which yields eigenvalues that are the negative reciprocals of the time constants of the system. In the case of large barriers (more than 4 kT), n distinct wells (states) yield n-1 significantly weighted "slow" eigenvalues, and TST kinetics are recovered complete with "shot" noise, i.e. diffusion theory predicts normal gating currents on the millisecond time scale. In addition, however, "fast" eigenvalues exist which correspond to rapid equilibration within wells. These produce gating current transients resembling early gating transients recorded experimentally with 200 kHz bandwidth resolution[1]. Aside from predicting high frequency events, the diffusion approach has the advantage that rates over barriers become diffusion limited as the barrier height decreases (e.g. large depolarizing pulses), preventing the endlessly increasing exponential rate constants that occur with TST. As more becomes known about the structural changes that occur with ion channel activation, the trend in modeling gating current kinetics will move away from mere phenomenological description in favor of models that reflect physical mechanisms. We feel that, given that ion channel activation appears to involve large scale displacement of charged domains through a condensed phase environment, diffusion theory is more appropriate than TST in characterizing gating charge movement. Supported by NIH GM30376.

1. Stefani and Bezanilla, this meeting, and (1996) *Biophys. J.*, 70(2): A143.

Tu-PM-C8

DIFFERENT APPARENT GATING CHARGES AMONG *SHAB* POTASSIUM CHANNELS.

((**Leon D. Islas** and Fred J. Sigworth)), Dept. Cell. and Molec. Physiology, Yale School of Medicine, New Haven, CT, 06520.

Shab family potassium channels have two fewer positive charges than *Shaker* in the S4 region and are thought to have less voltage sensitivity. We have previously shown, using the method of Patlak et al. (*J.G.P, 106,:1058-1068*) that a mammalian *Shab* homologue (Kv2.1) has a gating charge of 12 -13 e_0, as do *Shaker* channels and Kv1.1. Here we report similar measurements on the *Drosophila Shab* channel. The voltage dependence of *Shab* is consistent with a smaller charge of 7-8 e_0. This contrasts with the higher value in Kv2.1, even though the channels have the same charge content in the putative voltage sensor regions.

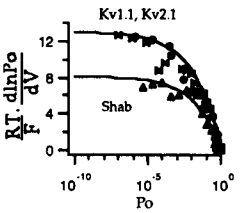

Tu-PM-C9

MODELS OF GATING CURRENT FLUCTUATIONS IN *SHAKER* K^+ CHANNELS. ((Y. Yang and F. J. Sigworth)) Department of Cellular and Molecular Physiology, Yale School of Medicine, New Haven CT 06520.

Discrete charge movements underlying gating currents give rise to nonstationary "shot" noise. A relatively well-constrained model for the gating process of Shaker K channels (N. E. Schoppa and F. J. Sigworth, submitted) underestimates the variance of gating current fluctuations. We are examining modifications to this and other models that may improve their descriptions of the fluctuations. The figure shows the mean current and time dependence of the variance from an ensemble of gating current responses from W434F-mutant *Shaker* channels with depolarizations to +40 mV.

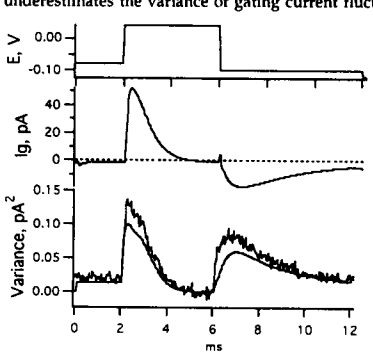

Tu-PM-D1

EFFECT OF SIZE AND SHAPE ON DIFFUSION OF MOLECULES IN MEMBRANES ((Cuihua Lui, Allison Paprica and **Nils. O. Petersen**)) Department of Chemistry, The University of Western Ontario, London, ON N6A 5B7

Diffusion of lipids in biological membranes is believed to be controlled by the free area at the membrane surface. The diffusion of large proteins in model membranes is better explained by hydrodynamic models. Protein diffusion in cells appear to be comparable to diffusion in model membranes except that they are often restricted to move in submicron domains. This work describes the diffusion characteristics of a series of lipid-like molecules for which the size and shape at the membrane surface have been increased systematically from 0.3 nm^2 to 2.4 nm^2 to bridge the gap between lipid diffusion and large molecule diffusion. The data confirm that diffusion depends on size and shows that the size-dependence can be modelled well by application of either Saffman-Delbrück or the Evans-Sackman hydrodynamic models for diffusion in two-dimensional thin films. The data suggest that the membrane is a dynamic structure with three layers: the region of about 10 nm from each surface is more rigid and controls the lateral diffusion of any molecule which penetrates partly into it while the region in the middle is very fluid and allows rapid diffusion unless parts of the molecule penetrates the more rigid layer. This triple layer model is completely consistent with the dynamic models derived from order parameters from nmr or esr experiments.

Tu-PM-D2

STRUCTURE AND PHASETRANSITIONS IN CATIONIC LIPID-OLIGONUCLEOTIDE CONDENSATES ((G. Kminek, R. Zantl, I. Sprenger, G. Rapp*, **J.O. Rädler**)) Institute for Biophysics E22, Technical University Munich, 85748 Garching, Germany, * EMBL c/o DESY, Notkestrasse 85, D-22603 Hamburg, Germany (Spon. by E. Sackmann)

Cationic liposomes complexed with plasmid DNA are highly efficient as gene carriers in eucaryotic cells. An essential feature of this transfection methode is that the liposomes when mixed with DNA collapse into dense liquid crystalline condensates. We investigated the structure and thermodynamic properties of aggregates of DMPC/DMTAP (dimyristoylphosphatidylcholin / dimyristoyl-trimethyl-ammonium propane) and 20bp doublestranded-oligonucleotides. The oligo-lipid condensates exhibit liquid crystalline order comprised of 2-dimensionally packed ds-oligos confined between lamellar lipid membranes. The mesoscopic morphology of the lamellar aggregates as observed by negative staining EM exhibits a fine mesh in contrast to lipid condensates with long (48kbp) λ-DNA, which forms polydisperse but distinct globules. The lipid chain melting and the DNA helix-coil phase-transitions was investigated by X-ray diffraction, DSC, FTIR and fluorescence spectroscopy. Also the adsorption of DNA on single substrate supported cationic bilayers as a function of salt concentration was measured using ATR-FTIR and fluorescence resonance energy transfer (FRET).

Tu-PM-D3

HEADGROUP MOBILITY AND MEMBRANE HYDRATION CAN BE DETERMINED FROM THE COMPOSED PARELECTRIC RESPONSE OF BIOLOGICAL MEMBRANES. ((**B.Klösgen**, Ch. Reichle, St. Kohlsmann and K. D. Kramer.)) Fachbereich Physik, Freie Universität Berlin, Arnimallee 14, D-14195 Berlin, Germany.

High resolution parelectric spectroscopy is performed by a newly developed microprobe in combination with a commercial network analyzer and an adequate software for measuring and analyzing. A low amplitude rf wave is swept in a range (1-1000)MHz and applied to a sample of stapled fully hydrated lipid membranes. Relaxation curves are obtained for both absorption and dispersion. Interpretation using modified Debye's equations revealed contributions of the headgroup and bound water molecules with either one distinct relaxation frequency or a weighed distribution reflecting to the shell-like hydration water structure. Distinct activation energies could be attributed to both relaxation processes. Phase transitions of the lipid bilayer result in a small but still observable step of the headgroup relaxation frequency. Parelectric spectroscopy can be applied as a tool to measure the effects of the differently relaxing dipoles even in a complex system like real biological membranes. The dielectric properties in these biological materials are accessible by our low cost and easily transportable small device. This makes the method promising for medical diagnosis. First experiments in much more complicated systems like whole cells and cell aggregates at least reveal an interpretation in terms of „normal" and „abnormal" behavior and have already been proved to be helpful.

Tu-PM-D4

LAMELLAR BIOGELS: FLUID MEMBRANES PARTIALLY COATED WITH POLYMER-LIPIDS ((**H. E. Warriner**, P. Davidson, N. L. Slack, M. Schellhorn, P. Eiselt, S. H. J. Idziak, H. W. Schmidt, C. R. Safinya)) University of California, Santa Barbara and Universitat Bayreuth, Germany

We report on X-ray, polarized light microscopy and rheometric studies of a liquid crystalline hydrogel, $L_{\alpha,\xi}$, discovered in multilamellar phases of fluid membranes coated with polymer-surfactants. The existence of the $L_{\alpha,\xi}$ has been demonstrated in mixtures of DMPC, pentanol, water and seven examples of PEG-surfactant (500, 2000 or 5000 g/mole polyethylene glycol covalently attached to the head of a double-chained surfactant).[1,2] For all seven PEG-surfactants, lamellae are in the fluid, chain-melted state, proving that the $L_{\alpha,\xi}$ is not a form of $L_{\beta'}$ gel. Also, unlike traditional polymer gels, less PEG-surfactant is required for gelation as water content increases. Comparisons between the different PEG-surfactants show that gelation is strongly dependent on polymer MW but independent of molecular details of the surfactant moiety. The $L_{\alpha,\xi}$ regime is characterized by a proliferation of layer-dislocation defects, probably stabilized by a segregation of PEG-surfactants to the defected regions. We propose that these defects, resisting shear in any direction, are the source of the gel-like elasticity and compare the predicted gel-transition curve to the experimentally obtained curves.

Work supported by NSF grants DMR-9624091 and DMR-91-23048, and the Petroleum Research Fund (No. 31352-AC7).

1. Warriner et al., *Science*, V. 271, 969 (1996)
2. Warriner et al., submitted to *J. of Chemical Physics*.

Tu-PM-D5

MECHANICAL ASPECTS OF MEMBRANE THERMODYNAMICS CLOSE TO LIPID MELTING TRANSITIONS ((**T.Heimburg**)) Max-Planck-Institut für biophysikalische Chemie, 37077 Göttingen, Germany

Heat capacity and isothermal compressibility are related to the fluctuations in enthalpy and volume, respectively. Close to the melting transition of lipid membranes enthalpy and volume fluctuations are proportional to each other and thus the heat capacity and the isothermal compressiblity are coupled in a simple manner. Similar statements can be made in respect to the isothermal area compressibility, the adiabatic compressibility and the bending rigidity of membranes. All of these susceptibilities can be approximated by simple functions of the heat capacity close to the main transition.

The close coupling of thermotropic and mechano-elastic properties of membranes allows for the interpretation of some interesting experimental findings.The critical behavior of the ultrasonic velocity at the lipid melting point and its frequency dependence can be obtained from calorimetric measurements. Furthermore the high lateral and bending elasticities in the lipid melting regime are explained. Finally, vesicles under osmotic stress are predicted to collapse close to transitions, due the increased bending elasticity, thus relating vesicular shapes to the lipid chain melting transition. This coupling gives rise to characteristic heat capacity profiles with more than one heat capacity maximum. Such a behavior has been found previously in an anionic lipid system that undergoes structural changes from vesicles to bilayer networks close to the melting transition under osmotic stress conditions (Heimburg & Biltonen, Biochemistry 33 (1994), 9477).

Tu-PM-D6

THEORETICAL PHASE DIAGRAMS FOR LIPID–CHOLESTEROL BILAYERS

Morten Nielsen,[1] Ling Miao,[2] John H. Ipsen,[2] Ole G. Mouritsen,[2] and Martin J. Zuckermann,[1]

[1]Physics Dept., McGill University, Montreal, QC, Canada;
[2]Chemistry Dept., Technical University of Denmark, Lyngby, Denmark

Lipid-cholesterol bilayers are modeled as two-dimensional systems of molecules with both translational and chain-conformational degrees of freedom. The translational variables of the molecules are represented by a *random* lattice whose configuration fluctuates. An additional variable is assigned to each lipid chain to describe its conformational states: either *ordered* or *disordered*, each having a different degeneracy. Finally, the interactions between the molecules are approximated by a hard-core repulsion and short-range attractions that depend not only on the chemical nature of the the interacting molecules, but also on their chain conformations. In essence, such interactions model cholesterol as an impurity, which tends to disrupt the lateral ordering of the lipid molecule and which prefers to be situated in the neighborhood of lipid chains in the ordered state. Monte-Carlo computer simulations of the model show that the decoupling of the order-disorder transition of the lipid chains from the lateral ordering of the system is induced by cholesterol and characterises the generics of the phase diagrams of such model systems.

Tu-PM-D7

PHOSPHOLIPID PACKING IN AN INTERDIGITATED BILAYER: A SOLID-STATE NMR STUDY. ((**Donald J. Hirsh**§, Jack Blazyk¶, and Jacob Schaefer§)) §Department of Chemistry, Washington University St. Louis, MO 63130 and ¶Department of Chemistry and College of Osteopathic Medicine, Ohio University, Athens, OH 45701

An analogue of dipalmitoylphosphatidylcholine (DPPC) which has a single fluorine at the methyl terminus of one fatty acid chain (F-DPPC) shows unusual behavior. The gel to liquid crystalline phase transition temperature of F-DPPC is 10 °C higher than that of DPPC. Phosphorous NMR indicates that the structures formed are lamellar. The solid-state NMR technique of REDOR, Rotational Echo DOuble Resonance, reveals that the fatty acid "tails" are in close proximity to the phospholipid head group. Overall, the NMR data for F-DPPC are consistent with a deeply interdigitated phospholipid bilayer. We are in the process of interpreting the observed intra- and inter-molecular dipolar couplings in terms of distance constraints. These will determine the conformation of F-DPPC and lipid packing in the interdigitated bilayer. The solid-state NMR technique of REDOR is a new approach to the characterization of membrane structure.

Tu-PM-D8

THERMOTROPIC BEHAVIOR AND RAMAN SPECTRA OF THE N-METHYLATED SERIES OF DIPALMITOYLPHOSPHATIDYL-ETHANOLAMINE (DPPE).

((O. Ruiz[1], D. Ramirez[1], T.J. O'Leary[2], and **J.A. Centeno**[2])) [1]University of Puerto Rico-Mayaguez, Chemistry Dept., Mayaguez, PR, [2]The Armed Forces Institute of Pathology, Dept. of Cellular Pathology (TJO), and Dept. of Environmental and Toxicologic Pathology (JAC), Washington, DC

Differential scanning calorimetry (DSC) and spontaneous Raman spectroscopy were employed to investigate the thermotropic behavior of the N-methylated series of dipalmitoylphosphatidylethanolamine (DPPE). Both the crystalline to liquid crystalline and gel to liquid crystalline phase transition temperatures (T_m) were established employing DSC. The Tms as determined by DSC were then used to guide the Raman study. Temperature profiles constructed from Raman spectra corresponding to the C-H stretching modes, the C-C stretching mode, and the intensity ratio of the CH_2 bending/CH_2 twisting deformation modes, were used to established bilayer conformational changes on these N-methylated lipids. Other changes associated with the glycerol carbonyl and the phosphate headgroup of the lipid were correlated with the number of methyl groups introduced at the $-CH_2CH_2NH_3^+$ moiety. The phospholipids studied were DPPE (C16:0), the monomethyl-(mDPPE) and dimethyl-substituted (dmDPPE). The thermotropic and spectroscopic properties of these DPPEs were compared with similar studies on DPPC (C16:0) and DMPE (C14:0) bilayers.

This study was supported by the American Registry of Pathology (Grant #2291 to JAC) and by NIH Grant 5 T34 GM08419-05 to Univ. of P.R.-Mayaguez.

Tu-PM-D9

GEL TO LIQUID CRYSTALLINE PHASE TRANSITION CHARACTERISTICS OF PHOSPHOLIPID BILAYERS ON A MICA SUPPORT. ((**R.F. Epand** and R.M. Epand)) Dept. of Biochemistry, McMaster University, Hamilton, Ontario, L8N 3Z5, Canada.

Oriented bilayers on solid supports are utilized in many studies of the structure and properties of membranes. These studies include diffraction, reflectometry, nuclear magnetic resonance, linear dichroism and atomic force microscopy. We have studied how the L_β to L_α phase transition of mica supported bilayers compares with those of multilamellar vesicles (MLV) of the same lipids. In the case of dipalmitoylphosphatidylcholine (DPPC), it is found that the P_β' to L_α transition temperature (T_m) is identical for the sample on mica but the enthalpy is reduced by about 30%. A possible cause of this effect is that interactions between mica and the flat morphology of the L_α phase is greater than that between the solid support and the rippled P_β' phase. Interestingly dimyristoylphosphatidylethanolamine (DMPE), a lipid that does not form ripple phases exhibits the same L_β to L_α transition enthalpy as MLV when deposited on a mica support. In addition the T_m of DMPE is raised 7° when placed on a mica support. There is evidence that phosphatidylethanolamines are not fully hydrated when oriented on a flat solid support which likely gives rise to the increase in T_m. Thus bilayers of different lipids are affected differently by being placed on a solid surface. These phenomena will contribute to a greater understanding of the relationship between the chemical structure of phospholipids and their physical properties.

Tu-PM-D10

Hexagonal Phase in POPC / $C_{12}EO_2$ Mixtures ((**S.S.Funari**)) Univ. Leipzig, Dept. of Physics. *present address*: MPI Colloids and Interfaces, c/o EMBL, Notkestrasse 85, D - 22603 Hamburg, Germany (sergio@embl-hamburg.de) (Spon. K. Brandemburg).

The phase diagram of the ternary system POPC/$C_{12}EO_2$/^2H_2O has been described before. It shows a wide variety of non-lamellar phases, indicating a rich balance of interactions between the components.

Neither the phospholipid POPC nor the non-ionic surfactant $C_{12}EO_2$, form a hexagonal phase in anhydrous form at different temperatures or in aqueous dispersions. However, mixtures of both at molar ratios between surfactant and lipid around $R_{wL} \sim 2$, do form an inverted hexagonal phase. This ratio coincides with a 1:1 number of alkyl chains between the amphiphiles. At lower R_{wL} one finds a gel phase, as seen in pure POPC while at higher R_{wL} there is a L_2 phase as in pure surfactant.

The interactions at the head group region play a vital role in the formation of such a phase. The hexagonal unit cell is sensitive to the amount of water present in the sample. For $R_{wL} = 2$ the interplanar repeat distance (10) ranges from 3.58 nm for a dry mixture to 4.33 nm at relative humidity RH= 0.75, which corresponds to cell parameters of 4.13 and 5.00 nm, respectively. I argue that the formation of the hexagonal phase is due to a stronger interaction of the lipid head group with EO than with water. This effect is enhanced by the need of the alkyl chains from the surfactant to be part of the hydrophobic core.

PROTEIN AND PEPTIDE CONFORMATION

Tu-PM-E1

CALMODULIN BINDS HIV-1 GAG AND p17.

((Wilson Radding, John P. Williams, Margaret A. McKenna, Eric Hunter, Ewan M. Tytler, Jay M. McDonald)) Department of Pathology, Atherosclerosis Research Center, and Center for AIDS Research, UAB, Birmingham, AL 35294.

Transfection of cells with vectors coding for the HIV-1 envelope glycoprotein, gp160, leads to increased cellular calmodulin in those cells which express gp160 (Radding, et al., BBRC 218:192-197,1996). The work pursued here rests on the premise that the calmodulin increase provides some advantage for the virus, possibly by providing calmodulin to interact with non-gp160 viral proteins. ^{125}I-calmodulin overlay studies show that calmodulin binds gag, the precursor of the viral structural proteins. The overlay studies also show that calmodulin binds p17, one of the proteolytic products of gag, but not p24, the gag product derived from amino acid sequence immediately C-terminal to that of p17. Fluorimetric analysis of the binding process using IAEDANS-calmodulin indicates that after the initial binding event there is a slow rearrangement. Structural studies prompted by this research may lead to new therapeutic approaches for amelioration of AIDS.

Tu-PM-E2

CONFORMATIONAL HETEROGENEITY IN HIV-1 NUCLEOCAPSID PROTEIN p7 ((**J.R. Casas-Finet**[1], M.A. Urbaneja[1], C. McGrath[1], R.J. Gorelick[1], W.J. Bosche[1], B.P. Kane[1], L.O. Arthur[1], L.E. Henderson[1], T. Copeland[2], B.M. Lee[3], R.N. De Guzman[3], M.F. Summers[3])) [1]AVP, SAIC Frederick, and [2]ABL-BRP, NCI-FCRDC, Frederick, MD 21702; [3]HHMI, UMBC, Baltimore, MD 21250. (Spon. by J.W. Erickson)

HIV-1 p7 is one of the cleavage products of the gag polyprotein precursor during virion maturation. p7 has two conserved sequences (zinc fingers, ZFs) that are involved in the binding of viral RNA. Frequency-domain fluorescence spectroscopy was applied to wt and mutated p7 proteins. p7 Trp lifetime was resolved into 3 exponential components. A long-lived τ_1 of 9.8 ± 0.2 ns ($\alpha_1 \approx 0.14 \pm 0.01$) and average $\langle\tau\rangle$ of 6.3 ± 0.1 ns were observed for wt p7 (res. 1-55), mutants with N-terminal truncations at residues 3, 7, or 10, and a peptide (res. 13-51) truncated at both ends. Long Trp lifetimes stem from rotationally hindered conformers of the indole ring. We attribute the 10 ns component to a close approach between F16 and W37, since it was not observed in mutants with the 1st ZF deleted or with a F16A point mutation. Mutants with metal cluster modifications (CCHH or CCCC) in both ZFs, swapped or duplicated ZFs exhibited intermediate effects ($\tau_1 \approx 6$ ns, $\langle\tau\rangle = 4.5$ ns). Apo p7 (either by Zn(II) chelation with EDTA, Cys alkylation or S-S formation) drastically reduced $\langle\tau\rangle$ to 2 ns. p7 Trp dynamic anisotropy was resolved into 3 rotational correlation times (θ). A θ_1 of 0.2 ns was assigned to indole ring flip; a θ_2 of 3 - 4 ns was attributed to segmental ZF mobility, whereas a long θ_3 would originate from p7 rigid-body motion. Both the long-lived τ and θ components were not observed in a 2nd ZF peptide (res. 34-51). Steady state Trp anisotropy decreased and became wavelength-independent for F16A p7, relative to wt p7, suggesting that the indole ring experiences lesser mobility and microenvironmental heterogeneity in the latter. ^{15}N-labeled wt p7 was studied by 600 MHz heteronuclear NMR spectroscopy. NOE data indicate interactions between the ZFs, consistent with the above model and previous findings of others [Morellet *et al.*, *EMBO J. 11*, 3059 (1992)]. However, the NOEs do not appear to be consistent with a single static structure. ^{15}N NMR relaxation studies reveal that the two ZFs have different rotational difussion properties, and indicate that the inter-finger NOEs are due to transient contacts. Average ^{15}N T_1/T_2 values yield a rotational correlation time of 3.5 ns, in agreement with fluorescence results. Constrained molecular dynamic simulations were carried out on a Cray J90 supercomputer. Structures were sampled at 1 ps intervals from a 300 ps dynamic trajectory, energy minimized and grouped into families. No unfavorable interactions between side chains in either the ZFs or the linker region precluded a close approach between F16 and W37. In summary, p7 exhibits conformational heterogeneity reflected in the occurrence of a transient structure, in which the two ZFs are in close proximity.

Tu-PM-E3

DIFFERENTIAL SUB-DOMAIN MOBILITY OF THE CATALYTIC SUBUNIT OF cAMP-DEPENDENT PROTEIN KINASE ((M. Gangal, S. Cox, J. Lew, T. Colman, M. J. Ashbacher, S. S. Taylor, and D. A. Johnson)) Div. Biomed. Sci., U. C., Riverside, Riverside CA 92521. (Spon. R. Zidovetzki)

Substrate binding to the catalytic (C) subunit of cAMP-dependent protein kinase induces large-scale structural changes which involve domain displacements and result in the closure (or partial closure) of the enzyme interdomain cleft. Because the magnitude of these domain displacements would dictate differential subdomain flexibility and suggest a role for these displacements in the catalytic process, we have begun to examine the subdomain mobility of the C subunit by measuring the time-resolved fluorescence anisotropy of a set of site-directed fluorescein (FM) labeled C subunits (K16C-FM, K81C-FM, I244C-FM, and N326C-FM). The anisotropy decay profiles of the K81C-FM (at the tip of the small lobe above the interdomain cleft) and I244C-FM (at the tip of the large lobe below the interdomain cleft) mutants are fairly similar to one another, two decay components one equal to the expected whole-body rotation correlation time (τ_c = 21 ns) and the other with a τ_c of about 1 ns, suggesting some mobility of the peptide backbones to which the probes are attached. The anisotropy decay of K16C-FM (in the A-helix on the back side) is single exponential and equal to the whole-body τ_c, suggesting that the peptide backbone to which fluorescein is attached is very much anchored to the main body of the protein. The anisotropy decay of N326C-FM (on the C-terminal tail) is biexponential with a fast component of about 3 ns and a slow component (≥30 ns) longer than the whole-body τ_c, possibly suggesting relatively slow movements of the peptide backbone.

Tu-PM-E4

FLUORESCENCE, PHOSPHORESCENCE, AND CIRCULAR DICHROISM CHARACTERIZATION OF THE TFE-INDUCED β-SHEET TO α-HELIX TRANSITION IN BOVINE β-LACTOGLOBULIN A. ((V Subramaniam*, D G. Steel and A Gafni)) The University of Michigan, Ann Arbor, MI 48109 *current address - Max Planck Institute for Biophysical Chemistry, D-37018 Gottingen, Germany.

β-lactoglobulin (β-LG) is a predominantly β-sheet mammalian milk protein. Recent reports on the effect of trifluoroethanol (TFE) on intact β-LG and on peptides derived from it have indicated a strongly cooperative transition from β-sheet to primarily α-helical structure; these results have been interpreted as indicative of non-hierarchical protein folding mechanisms. In the current study three independent parameters, CD, fluorescence, and the room temperature phosphorescence (RTP) decay of β-LG were used to study the effects of TFE. For TFE concentrations up to 15% (V/V) only a small increase in the characteristic α-helical CD signal at 222nm was found. A sharp cooperative transition from β-sheet to α-helical structure was, however, observed to occur between 15-20% TFE. Changes in the RTP decay rate and in the fluorescence vs. TFE concentration also indicate a cooperative transition coincident with the midpoint of the transition measured by CD. For TFE concentration in excess of 30%, the fluorescence spectrum and intensity approach those of β-LG extensively denatured in 6M GuHCL, suggesting that the β-sheet to α-helix conformational change exposes the two Trp residues in β-LG to the solvent. RTP lifetime, however, still shows the phosphorescent Trp to be shielded from water. It is interesting to speculate that a non-hierarchical folding intermediate is responsible for the biologically active but incompletely refolded state observed by us upon refolding extensively denatured β-lactoglobulin. (Supported by NIA AG09761).

Tu-PM-E5

MECHANISMS OF AMYLIN AGGREGATION AND ITS INHIBITION BY ALPHA CRYSTALLIN AND BY β-STRUCTURE DESTABILIZING AGENTS. ((E. Rhoades, J. Agarwal and A. Gafni)) The University of Michigan, Ann Arbor, MI 48109.

The formation, in pancreatic islets of Langerhans, of amyloid deposits composed of high molecular weight aggregates of the small β-cell secreted peptide amylin is one of the major pathologies associated with non-insulin-dependent diabetes mellitus (NIDDM). The factors which predispose some individuals for this aggregation are not clear, but a conversion of amylin to a predominantly β-structure is believed to be essential. In the present study a highly aggregatable fragment of human amylin was used to obtain mechanistic details on the aggregation, and to test potential strategies for its inhibition. When light scattering intensity of solutions of this peptide was followed vs. time, the aggregation kinetics was found to be sigmoidal with a long lag-phase followed by a rapid increase in aggregate-formation rate. The relative intensity of light scattering during this initial lag-phase indicates the presence of small aggregates early in the process, which may serve as nuclei for further aggregation. This observation is in line with recent reports that the alzheimer's amyloid beta protein forms micelles as the first step in its fibrillogenesis. When mole-stoichiometric amounts of the small heat-shock protein, α-crystallin, were added to amylin fragment samples, the aggregation was completely arrested; moreover, the light scattering intensity was reduced to levels which indicated the presence of monomeric peptide. Trifluoroethanol, a strong α-helix promoter, at 30% (V/V) concentration, had a similar inhibitory effect on the aggregation, demonstrating that when the conversion of this peptide to a predominantly beta structure is eliminated fibrillogenesis is arrested. (Supported by the Michigan Diabetes Research and Training Center.)

Tu-PM-E6

INFRARED AND CIRCULAR DICHROISM STUDIES OF NITROSYLATION IN PEPTIDES AND PROTEIN UNFOLDING IN APOMYOGLOBIN ((B. K. Mohney, E. T. Petri, and G. C. Walker)) University of Pittsburgh, Chevron Science Center, Pittsburgh, PA , 15260 (Spon. D. Beratan)

We report the infrared and circular dichroism signatures of nitroslyation in simple peptides and blood proteins. These thionitrites exhibit CD signatures at ca. 350 and 550 nm. Nitrosylation of cysteine residues perturbs amide infrared bands of the protein. This work aims to understand the delivery mechanism for highly reactive nitric oxide radical in biological systems.

We also report the static FTIR and uv-CD spectra of the temperature dependent conformational states of apomyoglobin in potassium phosphate and sodium acetate buffer solution at pH*=5.3 in D_2O. Difference spectra and global analysis of the amide I' region of the IR spectra reveal different hot and cold denaturated states. Cold denaturation leads to a molten globule state with an associated partial loss of helical structure identified at 1646 cm^{-1}. Heat denaturation also exhibits an absorption loss at 1646 cm^{-1} but leads to the appearance of aggregation at 1680 cm^{-1} and 1619 cm^{-1}. There is quantitative agreement of the ultraviolet circular dichroism and infrared estimates of protein helicity. Thermodynamic parameters for the denaturation have been estimated from the FTIR and CD data. pH dependent protein changes are also reported. Denaturation in potassium phosphate and sodium acetate are qualitatively similar although differences due to acetate anion binding to the protein are apparent between 40 and 70 °C. This work was supported by financial support from the Petroleum Research Fund and 3M Company through an Untenured Faculty Award .

Tu-PM-E7

Different protonation states of dipeptides probed by polarized Raman spectroscopy. ((Guido Sieler and R. Schweitzer- Stenner)) Institut für Experimentelle Physik, Universität Bremen, 28359 Bremen, Germany

Model peptides consisting of a single peptide group with different side chains and terminal groups serve as model systems for exploring the vibrational dynamics of larger peptides and proteins. In this study we have measured polarized Raman spectra (i.e. polarized parallel and perpendicular to the scattering plane) of Glycylglycine (DGL) and Acetylglycine (AGL) as function of pH. The data were taken with near UV-excitation (363 nm) to allow simultaneous detection of nearly all relevant bands contributing to the spectral region above 1200 cm^{-1}. The polarized spectra were normalized by utilizing the 934 cm^{-1} of sodium perchlorate which served as an internal standard and subjected to a thorough, self-consistent spectral analysis which allows the decomposition into even highly overlapping bands. The thus obtained results can be summarized as follows. 1.Amide I of both peptides consists of two subbands which result from vibrational mixing with the water bending modes of the aqueous environment. The intensities of these subbands redistribute at acid pH (1.5). This may result from the disrupture of hydrogen bonds between water and the carboxyl group due to the protonation of the latter. 2. For both peptides the intensities of Amide II, Amide III and a Raman band arising from the C-terminal's methylen bending mode decrease significantly with acid pH. This is likely to be caused by the elimination of the recently obtained $COO^- \rightarrow \pi^*$(peptide) charge transfer transition (Chen et al., JACS, in press, 1996) to which theses bands are vibronically coupled. For DGL, the intensities of Amide I, II and III are also reduced at pH=12. This may indicate that the deprotonation of the N-terminal changes the orientation of the carboxyl group which in turn affects orientation and oscillator strength of its charge transfer to the peptide.

Tu-PM-E8

FOLDING, DYNAMICS AND STRUCTURE OF THE NEUROPEPTIDE SUBSTANCE P FROM A 5.4-NS MOLECULAR-DYNAMICS SIMULATION IN WATER.
((G. Hummer and A. E. García)) Theoretical Biology and Biophysics Group T-10, MS K710, Los Alamos National Laboratory, Los Alamos, NM 87545. (Spon. by B. B. Goldstein)

The folding, dynamics and structure of the eleven-amino-acid peptide substance P in water is studied using a 5.4-ns molecular-dynamics simulation. Structure classes of substance P are determined from tree analysis based on root-mean-square distances and projections onto principal-component coordinates in conformation space. The central and C-terminal amino acids exhibit a high propensity to form an amphipathic helix that can serve as a receptor-binding motif. Non-specific hydrophobic and specific charge interactions can provide strong receptor binding of *oriented* substance-P molecules. Despite significant structural changes, the binding motif is conserved during the 5.4-ns trajectory. This increases the binding strength as the entropic cost of structural *freezing* is reduced.

Tu-PM-E9

M13 COAT PROTEIN: SUB–nm. HIGH RESOLUTION STRUCTURAL STUDIES OF A MEMBRANE EMBEDDED PEPTIDE – A SOLID STATE NMR APPROACH

((C. Glaubitz, G. Gröbner, A. Watts)) Department of Biochemistry, Oxford University, Oxford, OX1 3QU, Great Britain

The major coat protein of the filamentous *E. coli* bacteriophage M13 has the intriguing property of acting as a coat protein as well as an intrinsic membrane protein during the phage cycle. It is composed of three domains: a 20 residue N–terminal, a 19 residue hydrophobic core and a 10 residue C–terminal. The peptide can adopt an α–oligomeric or β–oligomeric form, as resolved by CD, FTIR and Raman spectroscopy, depending upon conditions used for incorporation into bilayers. Thus, this peptide can form two of the major transmembrane elements of larger integral membrane proteins. Two 52mer samples of M13 with two different ^{13}C spin pairs have been synthesized using the solid phase method. The peptide was reconstituted into dimyristoyl phosphatidylglycerol bilayers and studied using novel solid state NMR methods. Here we report highly resolved, sub–nm structural studies of three adjacent amino acids (Val29, Val30, Val31) in the middle of the transmembrane domain using *^{13}C rotational resonance MAS NMR*, in both conformations of the peptide. The orientation of these segments with respect to the bilayer normal has been studied in macroscopically oriented samples by *^{13}C static solid state NMR*.

With these results it will be possible to test structure prediction and optical spectroscopic methods which are currently employed to determine membrane protein structure as well as describe the peptide structure whilst membrane bound.

NUCLEIC ACIDS - CONFORMATION AND STRUCTURE II

Tu-PM-F1

Structural Basis for Slippage During DNA Replication: A Case Study of the Insulin-Linked Polymorphic Region.

Xiao Chen[1,2], Paolo Catasti[1,2], Robert K. Moyzis[3], E. Morton Bradbury[2] and Goutam Gupta[1]* [1]*Theoretical Biology and Biophysics,* [2]*Life Sciences Division,* [3]*Center for Human Genome Studies, Los Alamos National Laboratory, Los Alamos, NM 87545

The insulin-linked polymorphic region (ILPR), a tandem repeat of (ACAGGGGTGTGGGG)n·(CCCCACACCCCTGT)n, shows both intra and inter allelic variations in repeat length. In this work, we have examined whether formation of unusual structures by the G-rich and C-rich strand causes slippage during replication and the observed length polymorphism. In our replication assay, we insert defined lengths of (ACAGGGGTGTGGGG)n or (CCCCACACCCCTGT)n into the single-stranded M13 DNA template at *BamH1* restriction sites 40 bps downstream of the primer. We monitor the primer extension in presence of T4, T7, and *E. coli* DNA polymerases with or without the *E. coli.* single strand binding protein (SSB) and the human counter-part, RP-A. Under appropriate solution conditions, we observe replication arrests both for the G-rich and the C-rich strand in the template. The pattern of replication arrest indicates that the G-rich and the C-rich strand form multiply folded G-quartet and the C+C-paired i-motif structures even in presence of their complementary strands. The replication assay also reveals many finer details of these unusual structures: (I) The G-rich strands form an ordered array of hairpin G-quartet motifs for n≥6 at neutral pH. K^+ (and not Na^+) preferentially stabilizes this structure. Neither SSB nor RP-A can unwind the hairpin G-quartet structure and release the replication arrest although RP-A binds strongly to the single-stranded loop or the spacer region of the structure. (II) The C-rich strands form an ordered array of C+C-paired i-motifs for n≥6 at slightly acidic pH (<6.5). For repeat length 6, this structure can be unwound by SSB as evidenced by complete release of the replication arrest. However, we believe that for longer repeat lengths the i-motif structures will be more stable and will not be unwound by SSB or RP-A.

In summary, multiply folded G-quartet and the C+C-paired i-motif structures of the ILPR may cause slippage during replication and the observed length polymorphism.

Tu-PM-F2

GAA/TTC DNA Repeats Form Triplex Structures: A Possible Role in Friedreich's Ataxia. S.V. Santhana Mariappan, X. Chen, R.K. Moyzis, E.M. Bradbury and G. Gupta. Contribution from Theoretical Biology and Biophysics (T-10, MS K710), Life Sciences Division (LS-2, MS 880) and Center for Human Genome Studies, Los Alamos National Laboratory, Los Alamos, NM 87545.

Expansion of GAA/TTC triplet repeats (V. Campuzano et al. *Science* 271, 1423-1427) located inside the Friedreich Ataxia (FRDA) gene abrogates mRNA production and causes the associated disease. Here, we examine whether unusual DNA structures are involved in this disease. We carried out structural studies on $(GAA)_n$, $(TTC)_n$ and $(GAA)_n/(TTC)_m$ by NMR spectroscopy, gel electrophoresis, single-strand specific P1 enzyme digestion experiments and molecular dynamics simulations. $(GAA)_n/(TTC)_m$ (m=2n+1, 2n+2) form very stable triple helix structures under physiological solution conditions (Fig. 1A). An *in vitro* replication assay demonstrates the formation of the same triplex structure during replication of the $(TTC)_n$ template (Fig. 1B). The stability of the triplex structure is enhanced in longer repeat lengths implying that in disease phenotypes, the formation of triplex inside the intron may block chain elongation disrupting the mRNA production of the FRDA gene during transcription. In order to test this hypothesis, we carried out structural studies on the RNA-DNA hybrid sequences $(r(GAA)_n/d(TTC)_m)$. These sequences also form triplexes. A plausible model is proposed to explain the expansion mutation and the subsequent interruption of the replication machinery.

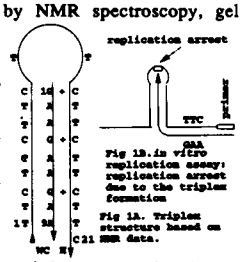

Tu-PM-F3

FRIEDREICH'S ATAXIA d(GAA) REPEATS FORM A HEAT-STABLE, NUCLEASE-RESISTANT STRUCTURE. ((**M. Christy**, I.-S. Suen, B.R. McEwen, I.S. Haworth, and M. Mitas)) Dept. of Biochemistry & Molecular Biology, Oklahoma State University, Stillwater, OK. 74078. Dept. of Pharmaceutical Sciences, Univ. of Southern California, Los Angeles, CA 90033.

At least ten human diseases [referred to as triplet repeat expansion diseases (TREDs)] are due to expansion of certain trinucleotide repeat sequences located within specific genes. The results of recent studies suggest that the sequences $[d(CTG)_n$, $d(CAG)_n$, $d(CGG)_n$ and $d(CCG)_n]$ associated with nine of the ten TREDs form hairpins, which has led to the hypothesis that hairpins play a role in expansion events. However, the recent discovery that d(GAA) repeats undergo expansion in the frataxin gene has cast a doubt on this hypothesis. To investigate the possibility that $d(GAA)_n$ contains secondary structure, the electrophoretic mobility of $d(GAA)_{15}$ was determined relative to its Watson-Crick form at 28 °C, pH 8.5. A single, non-protonated and unimolecular species of $d(GAA)_{15}$ was observed; its relative electrophoretic mobility (M_{rel}) was 0.94 [for comparison, the M_{rel} of the $d(CTG)_{15}$ hairpin = 1.12, while the M_{rel} of the $d(GAT)_{15}$ random coil structure = 0.88], indicating the presence of secondary structure. In contrast, the M_{rel} of the complementary sequence $d(TTC)_{15}$, which is predicted not to contain secondary structure, was 0.88. The T_m of $d(GAA)_{15}$ in 1 mM Na^+, determined from electrophoretic mobility melting profiles, was ~ 57 °C. Chemical modification of $d(GAA)_{15}$ with diethylpyrocarbonate and dimethyl sulfate revealed uniform reactivities of the adenines and guanines (respectively), indicating that the structure was not a hairpin. Although nucleotides flanking the d(GAA) repeats were hydrolyzed by single-strand-specific P1 nuclease, the triplet repeat region was refractory to the action of this enzyme at temperatures ≤ 65 °C. We suggest that d(GAA) repeats may adopt a stable helical-like structure that is not recognized by single-stranded DNA binding proteins required for replication and repair.

Tu-PM-F4

HYDRATION EFFECTS ON THE DUPLEX STABILITY OF PHOSPHORAMIDATE DNA-RNA OLIGOMERS ((Daniel Barsky*, Michael E. Colvin*, Gerald Zon†, Sergei M. Gryaznov†)) *Sandia Nat. Labs, Livermore, CA 94551-0969; †Lynx Therapeutics, Inc., 3832 Bay Center Place, Hayward, California 94545.

Recent studies on uniformly modified oligonucleotides containing 3'-NHP(O)(O⁻)O-5' internucleoside linkages (3' amidate) and alternatively modified oligonucleotides containing 3'-O(O⁻)(O)PNH-5' internucleoside linkages (5' amidate) have shown that 3' amidates duplexes, formed with DNA or RNA complementary strands, are more stable in water than those of the corresponding phosphodiesters. In contrast, 5' amidates do not form duplexes at all [S. M. Gryaznov *et al.*, Proc. Nat. Acad. Sci. 92(5798–5802), 1995]. There is no steric reason that the 5' amidate duplex should not form. We demonstrate that these differences arise from differential solvation of the sugar-phosphate backbones. By molecular dynamics calculations on models of 10-mer single-stranded DNA and double-stranded DNA-RNA molecules, both with and without the phosphoramidate backbone modifications, we show that the single-stranded 3' amidate and 5' amidate backbones are equally well solvated, but the 5' amidate backbone is not adequately solvated in an A-form duplex. These results are supported by quantum chemical free energy of solvation calculations which show that the 3' amidate backbone is favored relative to the 5' amidate backbone.

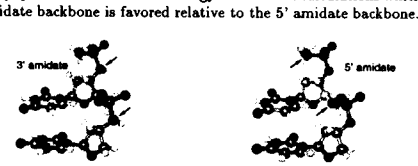

Tu-PM-F5

MOLECULAR DYNAMICS OF DNA DUPLEX WITH THYMINE GLYCOL ((N. **Luo** and R. Osman)) Dept. Physiology & Biophysics, Mount Sinai School of Medicine, New York, NY 10029

Endonuclease III of *E. coli* is a DNA repair enzyme which removes oxidized pyrimidines, such as thymine glycol, and cleaves apurinic/apyrimidinic (AP) sites. It has been proposed that a key step in the recognition of the damaged DNA is through an extrahelical thymine glycol which fits into a solvent pocket of the enzyme (1). NMR studies show that the thymine glycol is extrahelical (2), but the mechanism of base flipping is unclear. Base extrusion into an extrahelical position is studied by molecular dynamics simulations of a 13-mer DNA duplex, GCGCAGTgCAGCCG, with a thymine glycol in position 7. The solution structure of the damaged DNA containing a thymine glycol is distorted compared to normal DNA (3). The main distortions produced by the axial methyl of thymine glycol are characterised by an increase in the rise parameter and by weakening of hydrogen bonds in the vicinity of the damage. Such changes could facilitate extrusion of the damaged base. The structural changes in the DNA molecules with an extrahelical and an intrahelical thymine glycol serve to study the conformational as well as the energetic changes due to base flipping. In addition, the counterion distribution and the water structure around the damaged structures are investigated and compared with those of the undamaged DNA.

1. Thayer, M. M., *et. al. EMBO-J.* 14:4108-20 (1995).
2. Kao, J. Y., *et. al. J-Biol-Chem.* 268:17787-93 (1993).
3. Miaskiewicz, K., *et .al. Biopolymers.* 35:113-24 (1995).
Supported by USPHS Grant CA63317

Tu-PM-F6

THE PHENOMENON OF 2-D CONDENSATION OF DNA ON CATIONIC LIPID BILAYERS ((Jie Yang and Ye Fang)) Department of Physics, University of Vermont, Cook Building, Burlington, VT 05405.

It has already been established that the preparation of cationic lipid bilayers supported on the mica surface greatly facilitates high-resolution imaging of membrane-adsorbed DNA in solution with atomic force microscopy [1,2]. Our further study of the structure of DNA on supported cationic lipids indicates that the phenomenon is much more complicated than that of a simple adsorption of DNA onto a positively charged surface, and suggests that the behavior of DNA on cationic lipid bilayers is a 2-D condensation associated also with a dimensionality reduction [3]. In this report, we will present some results of our recent investigation of the 2-D condensation of DNA on cationic lipid bilayers. We will show that the lipid fluidity has a profound effect on the 2-D condensation of the membrane-adsorbed DNA. Ionic strength and ionic species also play some roles in arranging the condensed DNA. The interhelical distance of condensed DNA increases monotonically at the increase of the concentration of monovalent Na^+ ions. The effect of divalent ions and multivalent ions on the arrangement of condensed DNA is no longer monotonic and is more complicated.

1. Mou, J.; Czajkowsky, D.M.; Zhang, Y.; Shao, Z. FEBS Lett. **1995**, 371, 279.
2. Yang, J.; Wang, L.; Camerini-Otero, R.D. Nanobiology **1996**, in press.
3. Fang, Y, Yang, J. J. Phys. Chem. **1996**, in press.

Tu-PM-F7

ATOMIC FORCE MICROSCOPY OF SUPERCOILED DNA ((**Y.L. Lyubchenko** and L. S. Shlyakhtenko)) Department of Microbiology, Arizona State University, Tempe, AZ 85287-2701.

DNA supercoiling plays key roles in gene regulation, DNA recombination, repair and replication processes. To study conformation of supercoiled DNA in solution at different ionic conditions, we used atomic force microscopy (AFM) *in situ* . Supercoiled DNA molecules were imaged by AFM in solutions of different ionic strengths. The data obtained show directly and unambiguously that overall geometry of supercoiled DNA depends dramatically on ionic conditions. At low ionic strength DNA molecules have an irregular shape. Plectonemic superhelices are formed in high salt solutions. At such ionic conditions superhelical loops are often separated by the regions of tight helix-helix contacts. A high salt dependent mobility of tertiary structure of supercoiled DNA and formation of close contacts between DNA helices are important features of supercoiled DNA related to its biological functions.

ELECTRON TRANSFER SYSTEMS

Tu-PM-G1

VECTORIALLY-ORIENTED MONOLAYERS OF THE CYTOCHROME *C* / CYTOCHROME OXIDASE BIMOLECULAR COMPLEX. ((**Ann M. Edwards** and J. Kent Blasie)) Dept. of Chemistry, University of Pennsylvania, Philadelphia, PA 19104. ((John C. Bean)) Lucent Technologies, Murray Hill, New Jersey 07974.

Vectorially-oriented monolayers of yeast cytochrome *c* and its bimolecular complex with detergent-solubilized bovine heart cytochrome *c* oxidase have been formed by self-assembly from solution. Both quartz and Ge/Si multilayer substrates, the latter fabricated by molecular beam epitaxy (MBE), were chemical vapor deposited with an amine-terminated alkylsiloxane monolayer which was then reacted with a hetero-bifunctional cross-linking reagent - the resulting maleimide endgroup surface then provided for covalent interactions with the naturally occurring surface cysteine of the yeast cytochrome *c*. The bimolecular complex was formed by further incubating the cytochrome *c* samples in a cytochrome oxidase solution. The sequential formation of such monolayers and the oriented nature of the cytochrome oxidase was studied via meridional x-ray diffraction which directly provided electron density profiles of the protein(s) along the axis normal to the substrate plane. The nature of these profiles is consistent with previous work performed on either cytochrome *c* or cytochrome oxidase monolayers alone. Furthermore, optical spectroscopy has indicated that the rate of binding of cytochrome oxidase to the cytochrome *c* is an order of magnitude faster than the binding of cytochrome oxidase to an amine-terminated surface that was meant to mimic the ring of lysine residues around the heme edge of cytochrome *c* which are known to be involved in the binding of this protein to cytochrome oxidase. These vectorially-oriented monolayers of the bimolecular complex are now sufficiently well structurally characterized to undertake a number of related functional studies.

Tu-PM-G2

INTERMEDIATES IN THE REACTION OF CYTOCHROME *c* OXIDASE WITH DIOXYGEN. ((**Ólöf Einarsdóttir** and Artur Sucheta)) Department of Chemistry and Biochemistry, University of California, Santa Cruz, CA 95064.

The details of the mechanism of the reduction of dioxygen to water by cytochrome *c* oxidase, including the optical absorption spectra and the microscopic rate constants for all the steps involved, remain to be established. We have investigated the reaction of fully reduced cytochrome *c* oxidase with dioxygen using time-resolved optical absorption spectroscopy. Difference spectra were collected (λ = 370-720 nm) 50 ns to 50 ms after photolysis of the fully reduced CO-bound enzyme in the presence of dioxygen using a gated multichannel analyzer. Singular value decomposition (SVD) and multi-exponential fitting indicated the presence of six processes with apparent lifetimes of 1 μs, 10 μs, 26 μs, 32 μs, 86 μs and 1.3 ms. Using the SVD results and double difference maps, a sequential pathway with accompanying equilibria is proposed. Based on this mechanism, the time-dependent populations and difference spectra of the reaction intermediates, including those of the ferrous-oxy complex (compound A), peroxy and ferryl species, were determined. Compound A has a peak at 595 nm and a trough at 612 nm versus the reduced enzyme and reaches a maximum concentration at 30 μs. Cytochrome a_3 in the peroxy and ferryl derivatives has absorption maxima at 606 and 578 nm, respectively, versus its oxidized form. The difference spectra of these intermediates are analogous to those of P and F, obtained upon exposing the oxidized enzyme to a mixture of CO and O_2 or hydrogen peroxide, and provide unequivocal evidence for the presence of peroxy and ferryl intermediates during the dioxygen reduction by cytochrome oxidase at room temperature. Supported by NIH grant R29 GM45888.

Tu-PM-G3

INTERNAL ELECTRON TRANSFER AND OXYGEN REACTION IN WILD-TYPE AND HELIX-VIII MUTANTS OF CYTOCHROME *C* OXIDASE FROM *RHODOBACTER SPHAEROIDES*.

((P. Ädelroth, D.M. Mitchell^, R.B. Gennis^ & **P. Brzezinski**) Dept. Biochem. & Biophys., Göteborg Univ. & CTH, Medicinareg. 9C, S-413 90 Göteborg, Sweden; ^School of Chem. Sci., Univ. of Illinois, Urbana, IL-61801, USA)

Internal electron transfer (ET) and the oxygen reaction were studied in wild-type (WT) and mutant cytochrome aa_3 from *R. sphaeroides*. The mutated residues line a proton-transfer pathway proposed to be used by protons consumed during O_2 reduction (1). The turnover activities of the mutant enzymes were greatly reduced. In the absence of O_2, after flash photolysis of CO from the two-electron reduced WT enzyme, electrons are first transferred from heme a_3 to a ($\tau \cong 3$ µs), resulting in a ~40 % reduction of heme a. This equilibration is then followed by additional, slower ET from heme a_3 to a ($\tau \cong 1$ ms at pH 7), coupled to proton release to the medium. This reaction was modeled in terms of electrostatic interactions between heme a_3 and a protonatable group that changes its pK_a from 9.1 to 10.3 upon reduction of heme a_3 (2). In the mutant enzymes (T352A, T359A, K362M) the rate and extent of the rapid (3 µs) ET were not affected. However, in the T359A mutant enzyme the slower, proton-coupled ET was not observed. This shows that the mutation does not affect internal ET but impairs proton-transfer in which T359 is directly or indirectly involved. The reaction of the fully-reduced enzyme with O_2 was studied using the flow-flash technique. In the mutant enzymes ET rates associated with O_2 reduction were at most a factor of two slower, which indicates that residues T352, T359, K362 are not involved in proton transfer during oxidation but rather with reduction of the enzyme (3). (1) Iwata *et al.* (1995) *Nature* 376, 660; (2) Ädelroth *et al.* (1996) *Proc Natl Acad Sci* USA,93,12992; (3) Hosler *et al.*, (1996) *Biochem.* 35, 10776.

Tu-PM-G4

X-RAY STRUCTURAL STUDIES OF the MITOCHONDRIAL COMPLEX III DIMER FROM DIFFERENT VERTEBRATE SOURCES.

((**Edward Berry**, ZhaoLei Zhang, Li-Shar Huang, Young-In Chi, Sung-Hou Kim)) Lawrence Berkeley Laboratory, Berkeley, CA 94720.

We have crystallized complex III (the cytochrome bc_1 complex) in hexagonal($P6_522$) crystals from cow and rabbit, monoclinic($P2_1$) crystals from cow, and orthorhombic($P2_12_12_1$) crystals from chicken. The chicken crystals diffract to 3.0 Å, the hexagonal rabbit to 3.5 Å, and both cow crystals to 3.75 Å. Isomorphous phases from seven heavy atom derivatives of the orthorhombic crystals showed a dimer of the bc_1 complex in the asymmetric unit. This dimer map was used as a model for molecular replacement to phase the other 3 crystals. The molecular replacement phases were used to locate heavy atom sites in three derivatives of the beef hexagonal crystal, giving independent isomorphous phases for that crystal.

The monoclinic crystal also has a dimer in the asymmetric unit. In the hexagonal crystals the dimer axis is positioned on a crystallographic 2-fold axis, giving a monomer in the asymmetric unit. Because two of our crystals have a dimer in the asymmetric unit, we can address questions about possible asymmetry of the bc_1 dimer.

We have 6 crystallographically independent monomers (4 crystal forms, two with non-crystallographic symmetry). We are using multicrystal- and ncs- averaging for phase improvement and extension. At present we clearly see transmembrane helixes and iron centers. There is a significant difference in the ironsulfur position between the beef and chicken crystals. The distance from the ironsulfur center to cyt. c_1 is 21.5 Å in the chicken crystals and about 15 Å in the beef hexagonal crystals.

Tu-PM-G5

CHARACTERIZATION OF RIESKE [2FE-2S] PROTEIN MUTANTS AND REVERTANTS IN THE *RHODOBACTER CAPSULATUS* BC_1 COMPLEX. **((T. Ohnishi,** G. Brasseur, V. Sled, and F. Daldal)) Univ. of Pennsylvania, Philadelphia, PA 19104.

To further understand the functional role of the Rieske protein in the Q_o site catalysis, PS^+ revertants were selected from three PS^- Rieske mutants, L136D, R, G (L136 is next to a cluster His-ligand). Six distinct revertants were found: 2 reversions in the original position (L136A and Y), 1 reversion at position 44 (L136G + V44F) and 3 others at position 46 (L136G +A46P, V, T). The second site suppressors found in the N-terminal part of the protein show slower growth and electron transfer than the wild-type, and substoichiometric amount of Rieske protein. The g_x features and E_m of Rieske protein show affected Q/QH_2 binding or/and E_m. Some revertants show altered g_x response to stigmatellin. Moreover, all the revertants are stigmatellin resistant and myxothiazol hypersensitive *in vivo*. The fully conserved L136 sticks out of the protein in the 3D-structure [1] and is involved in sensing the redox state of the quinone pool, and inhibitors [2]. The single mutants V44F and A46T have unusually high E_m value (~380 mV), indicating that the N-terminal part of the Rieske protein interacts physically and functionally with its cluster region in the Q_o site of the bc_1 complex. [1] Iwata, S. *et al.* '96. Structure 4, 567. [2] Liebl, U. *et al.* '95, in Photosynthesis: from Light to Biosphere,II (Mathis, P., ed.), pp. 749, Kluwer Academic Publishers, Dordrecht (supported by NSF grant MCB94-18694 to T.O. by and NIH GM-38237 to F.D.).

Tu-PM-G6

COMPUTATIONAL STUDIES OF REDOX POTENTIALS OF RUBREDOXIN: ROLE OF SMALL, NONPOLAR RESIDUES IN PROTEIN ELECTROSTATICS. **((Robert B. Yelle, Paul D. Swartz and T. Ichiye)) Department of Biochemistry/Biophysics, Washington State University, Pullman, WA 99164-4660.**

Despite the ever growing number of crystallographic and NMR structures of electron transfer proteins, the molecular basis of different redox potentials for proteins with the same redox site often remains unclear. From recent computational and experimental studies of the iron-sulfur protein rubredoxin, small nonpolar residues unexpectedly appear to play important roles. For instance, a 50 meV difference between two groups of homologous rubredoxins can be explained by whether a certain residue is either a Val or a Ala. The slight size difference between the two causes a small shift in the backbone, which has a large effect on the electrostatic potential at the redox site because of the proximity of the backbone carbonyls and amides to the redox site. Also, Val or Ile at two residue positions in homologous rubredoxins have been identified as possible gates controlling the solvent accessibility of the redox site. The degree of solvent accessibility can greatly affect the redox potential via the large contribution of highly polar water molecules to the electrostatic potential at the redox site. Molecular dynamics and other computational studies of these phenomena will be described and compared to other recent mutational studies.

Tu-PM-G7

Substrate and Temperature Dependence of DNA-Photolyase Repair Activity Studied by Ultrafast Spectroscopy

((Z. Xiaodong[†], A. Sancar[†], P.F. Heelis[‖], G. Bieser[§], T. Langenbacher[§], R. Heinecke[§], C. Musewald[§], C. Kompa[§], F. Pöllinger-Dammer[§] and **M.E. Michel-Beyerle[§]**))

[†] Department of Biochemistry and Biophysics, University of North Carolina School of Medicine, Chapel Hill, NC 27599-7260, USA

[‖] Research Division, North East Wales Institute, Clwyd CH5 4BR, United Kingdom

[§] Institute of Physical Chemistry, TU Munich, Lichtenbergstraße 4, D-85748 Garching, Germany

UV-irradiation of DNA initiates dimerization of adjacent thymines. This damage can be photo-repaired by DNA-Photolyase. The cofactor responsible for this splitting of the dimer is a flavin in its reduced state $FADH^-$. The repair process has been traced by transient absorption spectroscopy with fs- to ps-time resolution at high and low temperatures (275 K– 90 K). The results can be summarized as follows: (i) The lifetime of $^1(FADH^-)^*$ depends not only on the presence of substrate but also on its nature, i.e. the electron transfer from $^1(FADH^-)^*$ to thymine dimers T<>T and to thymine-uracil dimers T<>U is slower by a factor of 2 - 3 as compared to U<>U and U<>T. This feature is attributed to the stronger electronic coupling between $^1(FADH^-)^*$ and U<>U in the absence of the methyl group in the C5 position of the 3'-uracil. (ii) The quantum yield of repair is temperature dependent and below 200 K no repair is observed. The activation energy for the repair process has been determined to be $E_a = 0.45 \pm 0.1$ eV. (iii) With the assumption that the decay of $^1(FADH^-)^*$ in the presence of substrate is due to electron transfer, the charge recombination rate of the unsplit dimer at *low temperature* has been estimated to be faster than $(200\ ps)^{-1}$. Since this value is also expected to be a lower limit for the charge recombination rate at *high temperature*, where the quantum yield of splitting approaches unity, this result allows for the first time conclusions on the rate of bond splitting which has to exceed the low temperature limit of charge recombination of $(200\ ps)^{-1}$considerably.

Tu-PM-G8

SUBSTRATE AND TEMPERATURE DEPENDENCE OF DNA-PHOTOLYASE REPAIR ACTIVITY STUDIED BY ULTRAFAST SPECTROSCOPY

((X. Zhao[†], A. Sancar[†], P.F. Heelis[‖], G. Bieser[§], T. Langenbacher[§], R. Heinecke[§], C. Musewald[§], C. Kompa[§], F. Pöllinger-Dammer[§] and **M.E. Michel-Beyerle[§]**))

[†] Department of Biochemistry and Biophysics, School of Medicine, University of North Carolina, Chapel Hill, North Carolina 27599

[‖] Faculty of Science, Health and Medical Studies, North East Wales Institute, Clwyd, UK

[§] Institute of Physical Chemistry, TU Munich, Lichtenbergstraße 4, D-85748 Garching, Germany

UV-irradiation of DNA initiates dimerization of adjacent thymines. This damage can be photo-repaired by DNA-Photolyase. The cofactor responsible for this splitting of the dimer is a flavin in its reduced state $FADH^-$. The repair process has been traced by transient absorption spectroscopy with fs- to ps-time resolution at high and low temperatures (275 K– 90 K). The results can be summarized as follows: (i) The lifetime of $^1(FADH^-)^*$ depends not only on the presence of substrate but also on its nature, i.e. the electron transfer from $^1(FADH^-)^*$ to thymine dimers T<>T and to thymine-uracil dimers T<>U is slower by a factor of 2 - 3 as compared to U<>U and U<>T. This feature is attributed to the stronger electronic coupling between $^1(FADH^-)^*$ and U<>U in the absence of the methyl group in the C5 position of the 3'-uracil. (ii) The quantum yield of repair is temperature dependent and below 200 K no repair is observed. The activation energy for the repair process has been determined to be $E_a = 0.45 \pm 0.1$ eV. (iii) With the assumption that the decay of $^1(FADH^-)^*$ in the presence of substrate is due to electron transfer, the charge recombination rate of the unsplit dimer at *low temperature* has been estimated to be faster than $(200\ ps)^{-1}$. Since this value is also expected to be a lower limit for the charge recombination rate at *high temperature*, where the quantum yield of splitting approaches unity, this result allows for the first time conclusions on the rate of bond splitting which has to exceed the low temperature limit of charge recombination of $(200\ ps)^{-1}$considerably.

Tu-PM-H1

INSIGHTS INTO THE MOLECULAR MECHANISM OF PORIN INHIBITION BY POLYAMINES. ((N. Liu, R. Iyer, H. Samartzidou and **A.H. Delcour**)) Department of Biology, University of Houston, Houston, TX 77204.

We have studied the modulation of two types of *E. coli* porins, OmpC and OmpF, by the polyamines putrescine (PUT), cadaverine (CAD), spermidine (SPD) and spermine (SPN). Both porins are inhibited by these compounds and show increased gating kinetics and stabilization of closed states. In both cases, the potency follows the series: SPN>SPD>CAD>PUT. The different polyamines also appear to affect porin gating in qualitatively distinct ways. OmpF is more sensitive than OmpC, especially to modulation by the larger compounds SPD and SPN. Modulatory effects can be observed when the drugs are applied to either sides of the membrane. This observation, in conjunction with the voltage-dependence of inhibition, suggests that the binding site is within the thickness of the membrane, possibly in the pore. We have compared the polyamine sensitivity of two OmpC mutants: the D118Q mutation, at the root of L3, had little effect of polyamine modulation, but the D105Q mutation, at the tip of L3, abolished the increase in closing frequency typically induced by polyamines. Both mutants however still showed modulation of opening kinetics. We propose that porins can exist under multiple closed and open conformations that are modulated by polyamines possibly binding at distinct sites. Preliminary experiments also indicate that the anionic-selective porin PhoE is much less sensitive to SPN than OmpC and OmpF. (Supported by NIH grant AI34905)

Tu-PM-H2

ONLY OLIGOMERIC FORMS OF LOW EFFICIENCY PORINS OMPA AND OPRF APPEAR TO CONTAIN OPEN CHANNELS. (E. Sugawara and **H. Nikaido**) Dept. of Molecular and Cell Biology, Univ. California, Berkeley, CA 94720-3206

The outer membrane proteins OmpA of *Escherichia coli* and OprF of *Pseudomonas aeruginosa* are homologous proteins that characteristically produce non-specific diffusion channels only at low efficiency. That is, a given amount of these proteins give, when reconstituted into liposome membranes, permeability to low molecular weight solutes that are about two orders of magnitudes lower than that produced by an equivalent amount of the classical trimeric porins such as OmpF, although their channel diameters are similar to, or even larger than, that of OmpF. We have shown earlier that only a small fraction of the OmpA population contains open channels (E. Sugawara and H. Nikaido, J. Biol. Chem. 269:17981, 1994). More recently, size fractionation of both OmpA and OprF populations has shown that the fractions at the leading edge of the peaks coming out of the gel filtration columns have a much higher channel-forming activity upon reconstitution into proteoliposomes. These results suggest that OmpA and OprF, which are normally folded as monomeric proteins, occasionally become folded as oligomeric proteins, and it is the latter that produces the characteristic low, inefficient permeability of porins of this class.

Tu-PM-H3

CHANNEL AND BIOCHEMICAL PROPERTIES OF BACTERIAL PORIN MUTANTS ((**Graeme Bainbridge**[1], Geoff A. Armstrong[1], Hamid Mobasheri[2], Edward J.A. Lea[2] and Jeremy H. Lakey[1])) [1]Department of Biochemistry and Genetics, The University of Newcastle upon Tyne, NE2 4HH, England, [2]School of Biological Sciences, UEA Norwich, NR4 7TJ, England.

Porins play a crucial rôle in the permeability properties of *E. coli* membranes and the three dimensional structure of several porins are now known. All show a similar fold: a β-barrel structure with long intrastrand loops on the extracellular side and short turns on the periplasmic side. All these porins also have an internal loop which forms the eyelet of the channel. This region has been shown to play a rôle in voltage gating *in vitro* (Jeremy H. Lakey, Edward J.A. Lea and Franc Pattus, FEBS Lett., **278**, 31-34, 1991) but controversy exists as to the rôle of the internal loop. We have cloned the OmpF porin gene from an *E. coli* B strain and used this construct to produce Cys, Ala and deletion mutants in the internal loop and the barrel wall. These channel mutants allow us to investigate the possible rôle the internal loop plays in voltage gating. Mutant porins have been expressed, purified and reconstituted into lipid bilayers. Channel and biochemical analysis will be presented.
This work is supported by the BBSRC grant # GR/J68809.

Tu-PM-H4

BACTERIAL PORIN CHANNELS AND VOLTAGE DEPENDENCE EXPERIMENTS WITH TWO BRUCELLA ABORTUS PORINS, ONE MISSING A 36 AMINO ACID SEGMENT. ((Hamid Mobasheri[1*], **Edward. J. A. Lea**[1], Thomas Ficht[3] Helene Marquis[4] and Jeremy H. Lakey[2])) [1]School of Biological Sciences, University of East Anglia, Norwich NR4 7TJ, UK, [2]Dept Biochemistry and Genetics, The Medical School, University of Newcastle, Newcastle on Tyne NE2 4HH, UK, [3]Department of Veterinary Pathobiology, Texas Veterinary Medical Center, Texas A&M University, College Station, Texas, TX77843, [4]University of Pennsylvania, School of Medicine, Department of Microbiology, 1033 Blockley Hall, Philadelphia, Pa19104

A number of bacterial porins exhibit channels of characteristic size and voltage dependence when incorporated into planar bilayer membranes. In particular, they close at high pd. and open at low pd .In a number of studies attention has been focussed on features of the β-strand structure which forms the channel and on the rôle of an intra-luminal loop common to many porins. Of the porins studied here, Omp2b and Omp2a , the latter is missing a 36 amino acid segment. From sequence analysis and topology prediction this deletion is likely to be in the intra-luminal loop. When incorporated into planar bilayers, both exhibit single channel behaviour . Omp2b exhibits single channels of approximately 300 pS in 1M NaCl, 10 mM $CaCl_2$, 10 mM Hepes, pH7.4. By contrast, Omp2a exhibits channels of a number of different sizes including 150, 250, and more rarely 600 pS as well as small ones of approximately 60 pS. Both Omp2b and Omp2a channels are voltage dependent, closing at high pd. and opening at low pd.These porins have been modelled using a procedure previously used for *E.coli* porins

*Supported by Ministry of Culture and Higher Education of the Islamic Republic of Iran.

Tu-PM-H5

HIGH-CONDUCTANCE BACTERIAL CHANNELS MAY MEDIATE THE TRANSLOCATION OF DNA ACROSS MEMBRANES ((I.Szabò, G.Bàthori, F.Tombola, M.Brini, A.Coppola and **M.Zoratti**)) CNR CS Biomembranes, Dept. Biomedical Sciences, Padova, Italy

The mechanisms by which genetic material crosses prokaryotic membranes are incompletely understood. When plasma membrane vesicles from the Gram-positive bacterium B.subtilis were fused into planar bilayers, we observed activity by high-conductance (nS range) channels, presumably the same already studied by us using the patch-clamp technique. In their presence, DNA could be translocated across the bilayer (as revealed by PCR amplification and Southern blotting) if a potential negative on the side of DNA addition was applied. Channel activity was modified by the presence of DNA, suggesting a block by molecules in transit. Translocation did not take place through the "empty" bilayer itself, or when the membrane contained Gramicidin A or a 30 pS anionic channel of eukaryotic origin. The results supportthe idea that transmembrane DNA transport in prokaryotes may proceed through bona fide channels.
(Supported by Telethon - Italy).

Tu-PM-H6

MOLECULAR DISSECTION OF THE LARGE MECHANOSENSITIVE ION CHANNEL (MscL) OF *E. COLI*. ((C.C. Häse[1,2], A.C. Le Dain[1] and **B. Martinac**[1])) [1]Dept. of Pharmacology, University of Western Australia, Nedlands, WA 6907, Australia, [2]Dept. of Microbiology and Molecular Genetics, Harvard Medical School, Boston, MA 0251, USA.

We have cloned several mutants of the *mscL* gene encoding the large conductance mechanosensitive ion channel (MscL) of *E. coli* into a glutathione S-transferase fusion protein (GST-MscL) expression system. The mutants had either amino acid additions, deletions or substitutions in the amphipathic N-terminal region, and/or deletions in the amphipathic central or hydrophilic C-terminal regions of the MscL protein. Proteolytic digestion of the isolated fusion proteins by thrombin yielded virtually pure recombinant MscL proteins that were reconstituted into artificial liposomes and examined for function by the patch-clamp technique. The addition of amino acid residues to the N-terminus of the MscL did not significantly affect channel activity, whereas N-terminal substitutions or deletions resulted in channels exhibiting altered pressure sensitivity. Deletion of 27 amino acids from the C-terminal region resulted in MscL protein that formed almost normal channels, while deletion of 33 C-terminal amino acids extinguished channel activity. Similarly, deletion of the internal amphipathic region of the MscL also abolished activity. In accordance with a recently proposed spatial model of MscL, our results suggest that (i) the N-terminal portion participates in the channel activation by pressure, and (ii) the essential channel functions are associated with both the putative central amphipatic α-helical region and the six C-terminal residues 104-109, RKKEEP, forming a charge cluster following the putative M2 membrane spanning α-helix.

Supported by the ARC grant A19332733 and a grant from the Raine Foundation.

Tu-PM-H7

RANDOM MUTAGENESIS OF A MECHANOSENSITIVE CHANNEL IDENTIFIES REGIONS OF THE PROTEIN CRUCIAL FOR NORMAL FUNCTION ((**Xiaorong Ou**, Paul Blount, Robert Hoffman, Ayumi Kusano, and Ching Kung)) Laboratory of Molecular Biology, University of Wisconsin-Madison, Madison, WI 53706

The *mscL* gene from *E. coli* encodes a peptide of 136 amino acids which forms a homohexameric complex that constitutes a functional mechanosensitive channel (MscL). This channel is thought to sense rapid decreases in environmental osmolarity and respond by release of intracellular small molecules and ions. To study the relationship between the structure and function of this channel, we have randomly mutagenized the *mscL* gene and isolated mutants that, when expressed, slow or halt growth. These are gain-of-function mutants since the *mscL* knockout shows no detectable plate phenotype. Thus far, over 20 mutants with single amino acid substitutions have been isolated. The majority and most severe mutations occur between amino acids 13 and 31, indicating the importance of this region in forming a proper channel. This region contains the first part of the first of two predicted transmembrane domains. Characterization of these mutants by whole cell physiology is now allowing us to sort them into different classes. For example, one class of mutants has lost the ability to retain the major osmolyte K^+ when the mutated gene is expressed, while another class increases K^+ efflux in response to osmotic shock. Preliminary electrophysiological data of mutants tested indicate changes in channel kinetics. Our results identify amino acid residues that are crucial for the proper functioning of this mechanosensitive channel. These data may also provide helpful information in elucidating the physiological role of the channel. (This study is supported by NIH GM47856)

Tu-PM-H8

BACTERIAL POLY(3-HYDROXYBUTYRATE) / POLYPHOSPHATE COMPLEXES FORM LARGE CONDUCTANCE CALCIUM CHANNELS. ((**Sudipto Das and Rosetta N. Reusch**)). Department of Microbiology, Michigan State University, East Lansing, MI 48824.

Complexes of short-chain poly(3-hydroxybutyrate) (PHB; MW~12,000) and inorganic polyphosphate (PPi; MW~5000), extracted from *Escherichia coli* plasma membranes, form ion channels in planar lipid bilayers that display many of the signal characteristics of calcium channels: voltage-activation, selectivity for divalent over monovalent cations, permeant to Ca^{+2}, Sr^{+2}, Ba^{+2}, and block by La^{+3}, Co^{+2}, Cd^{+2}, and Mg^{+2} in that order (Reusch et al. 1995. *Biophys. J.* **69**:754). The channel complexes have also been reconstituted from synthetic PHB_{128} and calcium $polyphosphate_{65}$ (manuscript in preparation).

The channels show a multiple number of substates and unique gating properties. Conductance of the most frequently observed open state is ~104 pS with frequent long openings of the order of several seconds. The channel complexes are impermeable to sodium and potassium. Pure synthetic PHB can form non-selective ion channels only at 100-1000 fold higher weight ratio in lipid (Seebach et al. 1996. *Helv. Chim. Acta* **79**:507). Analysis of open and closed time distributions reveal complex gating kinetics of the channel with multiple open and closed states. The single-channel characteristics in planar lipid bilayers of the biological and synthetic complexes are nearly indistinguishable.

Tu-PM-H9

HIGH RESOLUTION IMAGES OF MEMBRANE-ASSOCIATED STAPHYLOCOCCAL α-HEMOLYSIN OLIGOMERS BY ATOMIC FORCE MICROSCOPY. ((**Daniel M. Czajkowsky** and Zhifeng Shao))* Department of Molecular Physiology & Biological Physics and Biophysics Program, University of Virginia, Box 449, Charlottesville, VA 22908.

Staphylococcal α-Hemolysin (αHL) is a 34 kDa water soluble protein that forms pores in native and artificial membranes. The pores are believed to form when membrane-bound monomers convert into membrane-embedded oligomers during a multistep process. The oligomers, long thought to be hexamers, were recently shown to be heptamers on the basis of X-ray diffraction and gel shift experiments [Gouaux et al. *PNAS* 91, 12828 (1994)]. We have adapted a procedure which is frequently used to grow 2D crystals in electron microscopy to prepare αHL-loaded supported bilayers suitable for high resolution Atomic Force Microscopy in solution. Although Fourier transforms of the samples indicate better than 1 nm resolution, the size, shape, and subunit stoichiometry of the membrane-associated oligomers can be readily discerned even without applying image analysis techniques.
* This study was supported by grants from NIH.

Tu-PM-H10

STRUCTURE-BASED DESIGN OF A HETEROMERIC TRANSMEMBRANE PROTEIN PORE. ((**Orit Braha**[1], Barbara Walker[1], Stephen Cheley[1], John Kasianowicz[2], Michael R. Hobaugh[3], Langzhou Song[3], J. Eric Gouaux[3] and Hagan Bayley[1])) [1]Worcester Foundation, Shrewsbury, MA 01545; [2]NIST, Gaithersburg, MD 20899; [3]Columbia University, NY 10032. (Spon. C.N. Pace)

The ability to assemble, purify and reconstitute a heteromeric pore of known three-dimensional structure would be helpful in studies of the properties of transmembrane channels including permeation and gating. α-Hemolysin (α-toxin, αHL) is a 293-residue polypeptide secreted by *Staphylococcus aureus* as a water soluble monomer, which assembles into lipid bilayers to form a heptameric pore. Structure-based design and a separation method based on targeted chemical modification have been used to obtain a heteromeric form of αHL, $WT_6{}4H_1$. As modeled from the three-dimensional structure of WT_7, the 4H subunit contains an cluster of histidinyl residues that constitute a Zn(II)-binding site in the lumen of the transmembrane channel. The $WT_6{}4H_1$ heteromer was reconstituted into planar bilayers. Single channel currents through the heteromer are modulated by Zn(II), while currents through WT_7 are unaffected. The K_d for Zn(II) is ~ 200 nM and the k_{on} approaches the diffusion limit.

K CHANNELS AND DISEASE

Tu-Pos1

VOLTAGE-DEPENDENT KINETICS OF KVLQT1, A NOVEL DELAYED RECTIFIER K^+ CHANNEL. ((**M. Tristani-Firouzi**, P.S. Spector, A. Zou, M.T. Keating, M.C. Sanguinetti.)) Divisions of Cardiology and Pediatric Cardiology, University of Utah, Salt Lake City, UT 84113

KVLQT1 encodes a novel delayed rectifier K^+ channel. Mutations in *KVLQT1* cause an inherited arrhythmia, long QT syndrome. We recently demonstrated that KVLQT1 and minK coassemble to form I_{Ks} channels. KVLQT1 alone forms functional homomeric channels. The electrophysiological properties of KVLQT1 were studied in *Xenopus* oocytes. Activation of KVLQT1 current was best described by a 3 exponential function, accounting for an initial delay in current and fast and slow components of activation. The rates of activation were voltage dependent ranging from tau_f=154±9 and tau_s=762±57 msec at -10 mV to tau_f=47±2 ms and tau_s=272±10 ms at +40 mV. The relative amplitudes of the fast and slow components varied with membrane potential (fast: 0.22 at -20mV and 0.60 at +40mV; slow: 0.70 at -20mV and 0.26 at +40mV). Deactivating current was hooked when elicited after a pulse to membrane potentials > -30mV. This hook represents recovery of channels from an inactivated state at a rate faster than deactivation. The rate of recovery from inactivation and deactivation increased with increasing membrane potential: Deactivation: tau=70±4 ms at -130 mV; 775±53 ms at -50 mV (n=6). Recovery from inactivation: tau=14±2 ms at -130 mV; 70±5 ms at -50 mV (n=6). The voltage dependence of inactivation, estimated from the relative amplitudes of initial and extrapolated tail currents, was half-maximal at about -15 mV. These properties do not match any known human cardiac K^+ current, suggesting that KVLQT1 usually exists as a heteromultimeric channel in cardiac myocytes.

Tu-Pos2

OXIDATIVE STRESS MODULATES THE HUMAN ETHER-A-GOGO-RELATED GENE (HERG) K^+ CHANNELS

((P. Castaldo, F. Morra, S. Jossa, L. Annunziato and **M. Taglialatela**)) Section of Pharmacology, Department of Neurosciences, Faculty of Medicine, University of Naples Federico II, Via S. Pansini 5, 80131, Naples, Italy.

Oxygen radicals play an important role in arrhythmogenesis and contractile dysfunction in ischemia-reperfusion phenomena. The K^+ channel encoded by the human ether-a-gogo-related gene (HERG) appears to be a crucial molecular determinant for repolarization of the human heart. The aim of the present study was to investigate the modulation by oxidative stress of HERG K^+ channels expressed in Xenopus oocytes. Oxidative stress was induced by perfusion with a solution containing ferrous sulphate (100 μM) plus ascorbate (200 μM) (F/A solution). Oocytes perfused with ND88 (10 mM K^+) plus F/A showed a 10-fold increase in lipid peroxidation. Oxidative stress induced a 30-40% increase in outward K^+ current carried by HERG K^+ channels, without significant changes in inward current, thereby reducing inward rectification. The increase in both lipid peroxidation and HERG outward current started 2-3 min after the beginning of the F/A perfusion, reached a plateau within 6-8 minutes, and lasted for over one hour. Outward currents of uninjected oocytes were not affected by ND88 plus F/A perfusion. The increase in HERG outward currents was completely reversible upon removal of the ND88 plus F/A solution; a second exposure to F/A-containing ND88 induced another increase in outward currents, although slightly less pronounced than with the first application. Other K^+ channels were completely insensitive to oxidative stress (such as Kv 2.1) or only very slightly sensitive (<10% increase in outward currents, such as EAG). In conclusion, the inward rectification of HERG K^+ channels seems to be modulated by changes in the oxidative state of the cell.